The DNA Damage Response and Checkpoint Adaptation in *Saccharomyces cerevisiae*: Distinct Roles for the Replication Protein A2 (Rfa2) N-Terminus

Padmaja L. Ghospurkar,* Timothy M. Wilson,* Amber L. Severson,* Sarah J. Klein,† Sakina K. Khaku,† André P. Walther,† and Stuart J. Haring*,‡,1

*Department of Chemistry and Biochemistry and ‡Interdisciplinary Cellular and Molecular Biology Program, North Dakota State University, Fargo, North Dakota 58108, and †Department of Biological Sciences, Cedar Crest College, Allentown, Pennsylvania 18104

ORCID ID: 0000-0002-6169-3547 (S.J.H.)

ABSTRACT In response to DNA damage, two general but fundamental processes occur in the cell: (1) a DNA lesion is recognized and repaired, and (2) concomitantly, the cell halts the cell cycle to provide a window of opportunity for repair to occur. An essential factor for a proper DNA-damage response is the heterotrimeric protein complex Replication Protein A (RPA). Of particular interest is hyperphosphorylation of the 32-kDa subunit, called RPA2, on its serine/threonine-rich amino (N) terminus following DNA damage in human cells. The unstructured N-terminus is often referred to as the phosphorylation domain and is conserved among eukaryotic RPA2 subunits, including Rfa2 in *Saccharomyces cerevisiae*. An aspartic acid/alanine-scanning and genetic interaction approach was utilized to delineate the importance of this domain in budding yeast. It was determined that the Rfa2 N-terminus is important for a proper DNA-damage response in yeast, although its phosphorylation is not required. Subregions of the Rfa2 N-terminus important for the DNA-damage response were also identified. Finally, an Rfa2 N-terminal hyperphosphorylation-mimetic mutant behaves similarly to another Rfa1 mutant (*rfa1-t11*) with respect to genetic interactions, DNA-damage sensitivity, and checkpoint adaptation. Our data indicate that post-translational modification of the Rfa2 N-terminus is not required for cells to deal with "repairable" DNA damage; however, post-translational modification of this domain might influence whether cells proceed into M-phase in the continued presence of unrepaired DNA lesions as a "last-resort" mechanism for cell survival.

KEYWORDS Replication Protein A; DNA damage; checkpoint adaptation; phosphorylation; genetic interaction

CELLS encounter environmental stress on a continual basis and have evolved mechanisms to monitor the integrity of the genome and prevent temporary DNA lesions from becoming permanent DNA mutations. A central factor in genome monitoring is the protein complex Replication Protein A (RPA). The canonical RPA complex is composed of three subunits named RPA1, RPA2, and RPA3, also often referred to by their apparent molecular weights as RPA70, RPA32, and RPA14, respectively (Wold 1997; Iftode *et al.* 1999; Fanning *et al.* 2006; Zou *et al.* 2006; Oakley and Patrick 2010). Originally identified as a protein complex essential for *in vitro* SV40 DNA replication (Wold and Kelly 1988; Wold *et al.* 1989; Weinberg *et al.* 1990), this complex is also essential for DNA repair/recombination (Longhese *et al.* 1994; Firmenich *et al.* 1995; Sung 1997; Umezu *et al.* 1998) and has roles in cell-cycle regulation (Longhese *et al.* 1996; Lee *et al.* 1998; Anantha *et al.* 2008; Anantha and Borowiec 2009). This is consistent with the major biochemical function of RPA, which is high-affinity binding to single-strand DNA (ssDNA), an intermediate of replication, repair/recombination, and substrate for checkpoint activation (Smith *et al.* 2010; Flynn and Zou 2010; Mimitou and Symington 2011; Ashton *et al.* 2013).

doi: 10.1534/genetics.114.173211
Manuscript received December 1, 2014; accepted for publication January 9, 2015; published Early Online January 15, 2015.
Available freely online through the author-supported open access option.
Supporting information is available online at http://www.genetics.org/lookup/suppl/doi:10.1534/genetics.114.173211/-/DC1.
[1]Corresponding author: 1320 Albrecht Blvd., Burdick 322, Fargo, ND 58102. E-mail: stuart.haring@ndsu.edu

In addition to acting as a "sensor" of DNA damage through its ability to bind to ssDNA, RPA is also post-translationally modified in response to DNA damage. Identified post-translational modifications of RPA include acetylation (Choudhary *et al.* 2009), sumoylation (Burgess *et al.* 2007; Dou *et al.* 2010), and phosphorylation (Din *et al.* 1990; Dutta *et al.* 1991; Liu *et al.* 1995, 2005, 2012; Henricksen *et al.* 1996; Brush *et al.* 1996; Brush and Kelly 2000; Kim and Brill 2003; Vassin *et al.* 2004; Olson *et al.* 2006; Anantha *et al.* 2007, 2008; Lee *et al.* 2010; Shi *et al.* 2010; Wang *et al.* 2013). Most studies of RPA post-translational modifications have focused on hyperphosphorylation of the 40-amino-acid (aa) N-terminal region of human RPA2 in response to DNA damage. The use of "extensive" phospho-mutants (*i.e.*, those in which all serines/threonines in the region are changed to aspartic acids to mimic phosphorylation or alanines to prevent phosphorylation) indicates that mimicking a hyperphosphorylated state results in the inability to detect RPA2 foci at replication centers in otherwise unstressed human cells (Vassin *et al.* 2004). This suggests that in response to DNA damage, phosphorylated human RPA is recruited away from replication centers to perform functions in DNA repair. Mutagenesis studies have also indicated that phosphorylation of the human RPA2 N-terminus (NT) is important for halting the cell cycle during replicative stress (Olson *et al.* 2006), for progression into mitosis (Oakley *et al.* 2003; Anantha *et al.* 2008; Anantha and Borowiec 2009), and for differential protein interactions with some DNA-damage response proteins (Oakley *et al.* 2003, 2009; Patrick *et al.* 2005; Wu *et al.* 2005).

Within the human RPA2 NT are nine serine/threonine (S/T) residues that are targets for phosphorylation (Iftode *et al.* 1999; Anantha *et al.* 2007; Liu *et al.* 2012). The combination of various RPA2 phospho-mutants and the generation of phospho-specific human RPA2 antibodies have advanced this area of research by allowing for the examination of phosphorylation at each individual target residue. The sites in the human RPA2 NT appear to be differentially phosphorylated in response to various types of DNA damage (Liu *et al.* 2012), likely due to different checkpoint kinases (*e.g.*, ATR, ATM, and DNA-PK) having different preferential targets within the RPA2 NT (Brush *et al.* 1996; Olson *et al.* 2006; Cruet-Hennequart *et al.* 2008; Vassin *et al.* 2009; Liaw *et al.* 2011; Liu *et al.* 2012). Also, sequential phosphorylation of the human RPA2 NT has been reported, indicating a dependence on phosphorylation of one site to promote phosphorylation of another (Anantha *et al.* 2007; Liu *et al.* 2012). Although it is clear that many sites are differentially phosphorylated, the mechanism(s) by which post-translational modification of each site contributes to human RPA function in response to DNA damage remains undefined.

Recent examination of phosphorylation of Replication Factor A (RFA; yeast RPA) in the pathogenic yeast *Candida albicans* demonstrated that Rfa2 phosphorylation occurs both during the cell cycle and in response to DNA damage (Wang *et al.* 2013; Gao *et al.* 2014), similar to findings in *Saccharomyces cerevisiae* (Din *et al.* 1990; Brush *et al.* 1996; Bartrand *et al.* 2004). Dephosphorylation of *C. albicans* Rfa2 requires the Pph3–Psy2 phosphatase complex (Wang *et al.* 2013; Gao *et al.* 2014), and the PP2AC and PP4C phosphatases are necessary to dephosphorylate human RPA2 during the DNA-damage response (Feng *et al.* 2009; Lee *et al.* 2010). Mass spectrometry analysis of proteins isolated from unstressed *C. albicans pph3*Δ mutant cells revealed five potential targets of phosphorylation in Rfa2, none of which were located within the first 40 amino acids. Upon treatment of *Candida* cells with hydroxyurea (HU), it was determined that T11, S18, S29, and S30 in the Rfa2 NT are targets of phosphorylation by the yeast checkpoint kinase and ATR homolog, Mec1 (Wang *et al.* 2013; Gao *et al.* 2014).

In the budding yeast *S. cerevisiae*, post-translational modifications of Replication Factor A have been observed in response to DNA damage. Similar to human RPA1, yeast Rfa1 and Rfa2 are sumoylated in response to treatment of cells with methyl methanesulfonate (MMS) (Burgess *et al.* 2007; Cremona *et al.* 2012; Psakhye and Jentsch 2012). Phosphorylation of yeast Rfa1 at serine 178 (S178) and Rfa2 at serine 122 (S122) by Mec1 has also been observed in response to chemically induced DNA damage during mitosis (Brush *et al.* 1996, 2001; Brush and Kelly 2000; Bartrand *et al.* 2004). Furthermore, Rfa2–S122 is phosphorylated in response to programmed double-strand break (DSB) formation during meiosis (Brush *et al.* 2001; Bartrand *et al.* 2006). Yeast Rfa2 can also be phosphorylated at serine 27 (S27) by the meiosis-specific kinase Ime2 (Clifford *et al.* 2004, 2005), and it has been suggested that other unidentified residues in the N-terminus are also post-translationally modified during meiosis (Clifford *et al.* 2004). Rad53-dependent phosphorylation of the *Saccharomyces* Rfa2 NT has been observed in mitotically growing cells; however, this phosphorylation is observed only in a *set1*Δ mutant. Global mass-spectrometry analyses thus far have confirmed phosphorylation of Rfa1–S178 and Rfa2–S122 and have revealed other phosphorylation target sites (Rfa1–S160; Rfa2–T38, S115, S116, Y120, S189; Rfa3–S34; http://www.phosphogrid.org; Smolka *et al.* 2007; Albuquerque *et al.* 2008; Holt *et al.* 2009; Gnad *et al.* 2009; Helbig *et al.* 2010; Stark *et al.* 2010; Soulard *et al.* 2010), although the biological significance of each has yet to be determined.

In this study, the function of the *Saccharomyces* Rfa2 NT in the DNA-damage response was examined through a detailed genetic analysis of this region. It was determined that the *Saccharomyces* Rfa2 NT is necessary, yet its phosphorylation is not required for a proper DNA-damage response. Although phosphorylation is not required, a constitutive phospho-mimetic form of Rfa2 resulted in sensitivity to DNA damage. Genetic interaction analyses indicate that the basis for this sensitivity is different from the Rfa2 mutant lacking this domain. Utilizing multiple mutant forms of yeast Rfa2, specific subregions of the Rfa2 NT important for the damage response were identified. Finally, although Rfa2 phospho-mutants do not obviously affect initiation of checkpoint function, the phospho-mimetic form of Rfa2 displayed

genetic interactions and a checkpoint adaptation phenotype (*i.e.*, release from the G2/M checkpoint in the presence of unrepaired DNA damage) similar to that observed for *rfa1-t11* mutant cells.

Materials and Methods

Strains and plasmids

Yeast strains and plasmids used in this study are described in Supporting Information, Table S1, and Table S2, respectively. The yeast strains RMY122-A (*MATa leu2-3,112 trp1-1 can1-100 ura3-1 his3-11,15 rad5–G535R rfa1*Δ::*TRP1 rfa2*Δ::*TRP1*) and RMY122–*mre11*Δ were used to measure viability after plasmid shuffle and after DNA-damage treatment and are derivatives of W303 (Maniar *et al.* 1997; kindly provided by Steve Brill). These strains also contain a centromeric vector, pJM132 (pRS416 derivative), which includes the wild-type *RFA1*, *RFA2*, and *RFA3* genes expressed from their native promoters. All strains used for adaptation studies are derivatives of JKM179 (Lee *et al.* 1998; kindly provided by Jim Haber).

To generate a yeast shuttle vector containing wild-type *RFA1* and its native promoter, pJM132 was digested with *Bam*HI and *Hin*dIII, and this 2.6-kbp fragment was cloned into pRS313 (Sikorski and Hieter 1989) to generate pRS313–*RFA1*. The vector pKU2–*rfa1-t11* (Umezu *et al.* 1998), containing the *rfa1-t11* (K45E) mutation, was digested with *Age*I and *Hin*dIII, and this 2.0-kbp fragment was cloned into pRS313–*RFA1* to generate pRS313–*rfa1-t11*.

A yeast shuttle vector containing wild-type *RFA2* and its native promoter was generated as follows. *RFA2* cDNA was removed from pGDB-C3–*RFA2* by cleaving with *Eco*RI and *Hin*dIII (partial digest), and this 0.9-kbp fragment was cloned into the low-copy centromeric vector pRS315 (Sikorski and Hieter 1989) to generate pRS315–*rfa2*-Δpromoter (note that this plasmid contains a serine instead of a threonine at residue 3 of Rfa2). To amplify the native *RFA2* promoter, PCR was performed on pJM218 (Maniar *et al.* 1997) using primers –PR-R1 and –PR–*Nco*I. The resulting fragment was digested with *Sac*II and *Nco*I and cloned into pRS315–*RFA2*-Δpromoter to generate pRS315–*RFA2*.

N-terminal phospho-mutant forms of the *RFA2* gene were generated as follows. The plasmid pGDB-C3–*rfa2-D*$_x$ was constructed by annealing five overlapping complementary primers (AspA-E; Table S3), followed by insertion of this fragment into pGDB-C3–*RFA2* partially digested with *Eco*RI–*Hpa*I. The partially digested 0.9-kbp *Eco*RI–*Hin*dIII fragment from pGDB-C3–*RFA2* was then cloned into pRS315 to generate pRS315–*rfa2-D*$_x$-Δpromoter. The native *RFA2* promoter was amplified as described previously, digested with *Sac*II and *Nco*I, and cloned into pRS315–*rfa2-D*$_x$-Δpromoter to generate pRS315–*rfa2-D*$_x$. To generate pGDB-C3–*rfa2-A*$_x$, five overlapping complementary primers (AlaA-E; Table S3) were annealed followed by insertion into the *Nco*I and *Hpa*I sites of pGDB-C3–*rfa2-D*$_x$. Again, the 0.9-kbp *Eco*RI–*Hin*dIII fragment produced by partial digestion of this plasmid was cloned into pRS315 to produce pRS315–*rfa2-A*$_x$-Δpromoter. The PCR fragment containing the native *RFA2* promoter was digested with *Bam*HI and *Nco*I and inserted into pRS315–*rfa2-A*$_x$-Δpromoter to generate pRS315–*rfa2-A*$_x$. Deletion of the N-terminus of *RFA2* was achieved by PCR amplification of *RFA2* cDNA from pJM218 with a primer in which the codon for amino acid 39 was replaced with a start codon contained within an *Nco*I site. The resulting PCR product was digested with *Nco*I and *Hin*dIII and ligated into pRS315–*rfa2-D*$_x$ to generate pRS315–*rfa2*-Δ*N*$_x$.

Yeast integrating plasmids were also generated for each of the *rfa2* N-terminal mutant forms. Briefly, the 1.2-kbp *Bam*HI–*Hin*dIII fragment from pRS315–*rfa2-D*$_x$ and pRS315–*rfa2-A*$_x$ were each cloned into pRS306 to generate pRS306–*rfa2-D*$_x$ and pRS306–*rfa2-A*$_x$, respectively. These plasmids were then digested with *Eco*RI to target integration into JKM179, and two-step gene replacement was performed to generate *rfa2-D*$_x$ or *rfa2-A*$_x$ mutant strains. Double-mutant derivatives of JKM179 were generated by crossing isogenic strains, followed by sporulation and microdissection.

The construction of all individual and multimutant plasmids was performed using pAW7 as the original DNA template. Briefly, *in vitro* site-directed mutagenesis using *Phusion* DNA Polymerase (New England BioLabs) and the corresponding mutagenic primer listed in Table S3 were performed. Following *Dpn*I digestion, the mutagenesis reaction was transformed into bacterial cells. Plasmid DNA was isolated from resulting colonies and each mutation was verified by restriction digestion and sequencing.

Assessing the viability and recovery of rfa2 N-terminal mutants by plasmid shuffle

Centromeric plasmids containing various forms of *RFA1* (pRS313 derivative; *HIS3*) and *RFA2* (pRS315 derivative; *LEU2*) were cotransformed into RMY122-A or RMY122–*mre11*Δ cells. Transformants were selected on synthetic complete (0.5% ammonium sulfate, 0.17% yeast nitrogen base without amino acids) media containing 2% dextrose and lacking histidine, leucine, and uracil (SD–His–Leu–Ura), resulting in cells that contained three plasmids. Cells were grown in media (SD–His–Leu) selecting for the cotransformed vectors containing *RFA1* and *RFA2* alleles. If the allelic forms of *RFA1* or *RFA2* support growth, the pJM132 vector can be lost, and these cells can be recovered on media containing 0.8 μg/ml 5-fluoroorotic acid (5-FOA). If the allelic forms of *RFA1* and/or *RFA2* cannot support growth, no 5-FOA-resistant cells can be recovered. Finally, if there were synthetic growth defects due to the allelic forms of *RFA1* and/or *RFA2*, reduced loss of pJM132 (and a reduced number of 5-FOA-resistant cells) or slower growth of colonies on 5-FOA media is observed.

To assess the viability of *RFA1* and/or *RFA2* allele mutants, cells containing all three plasmids were grown in SD–His–Leu media overnight (16–24 hr) at 30° at 220 rpm. The next day, cells were counted and diluted to an initial

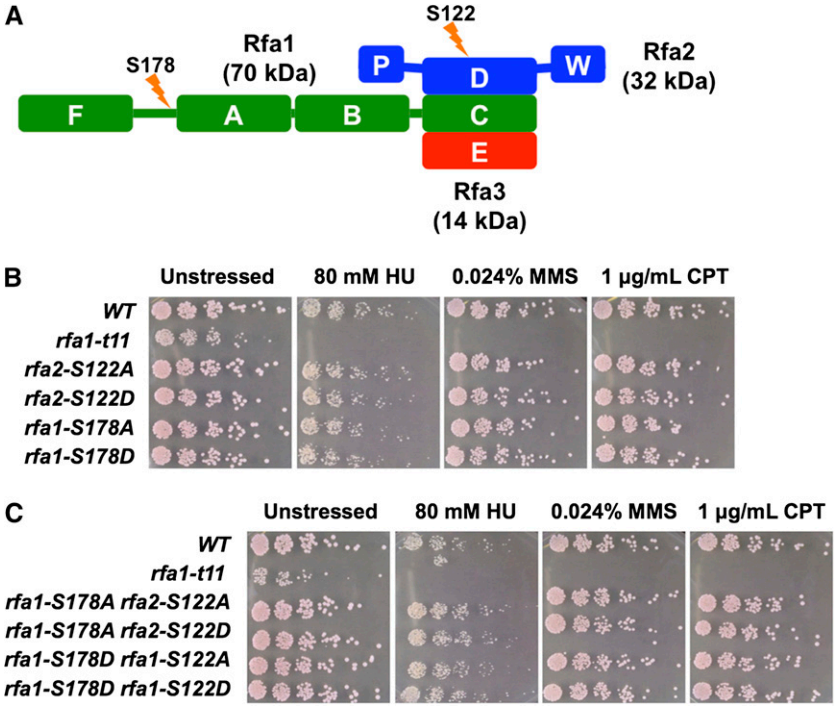

Figure 1 DNA-damage assay of known phosphorylation site mutants. (A) Schematic of RFA complex and individual subunits. The DNA-binding domains (DBDs) of the RFA subunits are shown (F, A, B, and C in *Rfa1*; D in *Rfa2*; E in *Rfa3*), along with linker regions (designated by thick lines connecting DBDs and other regions), the putative C-terminal winged-helix domain (W) of Rfa2, and the putative N-terminal phosphorylation domain (P) of Rfa2. Mec1 damage-dependent target sites are denoted by a lightning symbol, with the target residue (*e.g.*, S) and residue number (*e.g.*, 178) denoted. (B) DNA-damage assays of *rfa2-S122* and *rfa1-S178* mutants. Alanine, A, or aspartic acid, D, mutant forms were examined in this study. Cells were grown overnight, sonicated, counted, and diluted to 2.4×10^5 cells/ml. Threefold serial dilutions were made, and 5 µl of each dilution were spotted onto YPD (unstressed) or YPD containing 80 mM hydroxyurea (HU), 0.024% methyl methanesulfonate (MMS), or 1 µg/ml camptothecin (CPT). Plates were incubated for 2–4 days at 30°. The *rfa1-t11* strain was used as a control for DNA-damage sensitivity. (C) DNA-damage assays of *rfa2-S122* and *rfa1-S178* double mutants. Damage assays were performed as described in Figure 1B.

concentration of 1×10^6 cells/ml. Tenfold serial dilutions were made, and 5 µl of cells from the initial concentration and serial dilutions were spotted onto SD–His–Leu and 5-FOA plates, and 50 µl of the initial dilution were also spread onto 5-FOA plates. Growth was compared on the 5-FOA plates and quantitated. From the 5-FOA spread plates, we recovered mutant strains that were used in further studies.

Measuring growth rates of mutant strains

Yeast cells were grown overnight at 30° in 25–50 ml YPD (1% yeast extract, 2% peptone, 2% dextrose). The absorbance at 600 nm was measured to ensure that cells were in exponential phase ($OD_{600} < 2$). Cells were then diluted to $OD_{600} = 0.1$ in 50 ml YPD, measured to verify the initial concentration (OD_{600}), and grown at 30°. After 6–8 hr, the final concentration (OD_{600}) was measured. Growth rate (g; minutes per generation) was then calculated using the equation

$$g = t/\left[\ln\left(C_f/C_i\right)/\ln(2)\right],$$

where t is the time of growth, C_f is the final concentration of cells, and C_i is the initial concentration of cells. Measurements were taken for at least three independent cultures.

DNA-damage spot assays

Mutant strains that were viable were recovered as described above. These mutant strains were subjected to DNA-damaging agents as follows. Wild-type or mutant cells were grown in liquid YPD overnight (16–24 hr) at 30° at 220 rpm. The next day, cell concentrations were determined, and an initial dilution of cells to 2.4×10^5 cells/ml was made. Threefold serial dilutions were performed, and 5 µl from the initial dilution and serial dilutions were spotted onto the following plates: YPD, YPD + 0.012–0.03% MMS, YPD + 0.2–25 µg/ml camptothecin (CPT), YPD + 40–360 mM HU, YPD + 0.2–25 µg/ml phleomycin (PHL), and SD–His–Leu. Plates were incubated for 2–4 days at 30°, and growth differences between the mutant and wild-type cells were documented.

Immunoblotting

For protein analysis, wild-type and mutant cells were grown in liquid YPD media overnight (12–16 hr) to a concentration of $\sim 1 \times 10^7$ cells/mL. The next day, cells were subcultured into fresh media to a concentration of $\sim 2.5 \times 10^6$ cells/ml and grown for two generations. The cell cultures were split into two cultures, and MMS was added to one of the cultures to a final concentration of 0.03%. The cultures with/without MMS were grown at 30° for an additional 3 hr. For protein extraction, $\sim 3 \times 10^7$ cells were collected and treated as described by Kushnirov (2000). The samples were incubated at 100° for 3 min and centrifuged at 21,000 × g for 1 min, and the indicated amounts of the supernatant were loaded onto SDS–PAGE gels (described below).

To detect Rad53 activation (*i.e.*, phosphorylation), we loaded 10 µl (out of 100 µl) of sample onto a 6% SDS–polyacrylamide (37.5:1 mono:bis) mini gel. Following electrophoresis and transfer to 0.4-µm nitrocellulose, the blot was blocked with 10% skim milk in TBS-T for 1–2 hr, followed by primary antibody incubation with rabbit polyclonal anti-Rad53 (Abcam) at a 1:6,000 dilution in 10% skim milk for 16–20 hr. After multiple washes with TBS-T, the blot was incubated with goat anti-rabbit IgG-HRP secondary antibody (Abcam) at a 1:40,000 dilution in 10% skim milk for 2 hr. The blot was washed multiple times and developed using the ECL2 Western Blotting Substrate

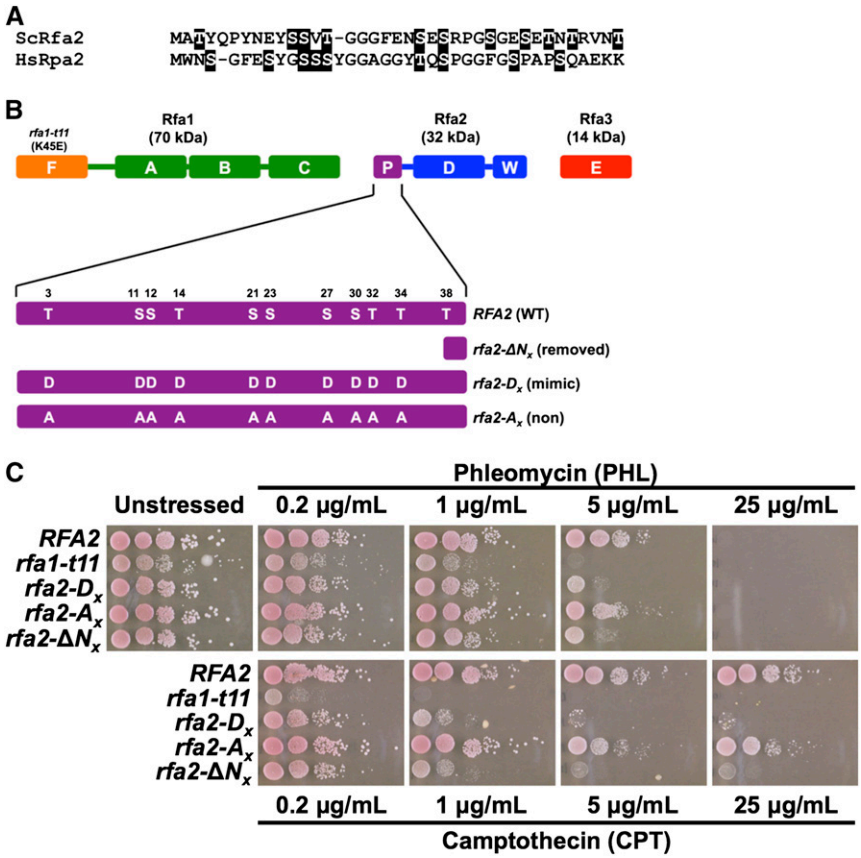

Figure 2 Phenotypic analysis of *rfa2* "extensive" (*rfa2*$_x$) mutants. (A) Alignment of RPA2 N-terminal regions (first 38 aa) from *S. cerevisiae* (ScRfa2; NP_014087.1) and *Homo sapiens* (HsRPA2; NP_002937.1). Alignments were performed using T-Coffee (suitable for small alignments) with default settings. Highlighted residues indicate putative phosphorylation sites in *S. cerevisiae Rfa2* and known phosphorylation sites in *H. sapiens* RPA2. (B) Schematic of *rfa2*-extensive mutants used in this study. Designations for domains are as described in Figure 1A. Serine/threonine amino acid (aa) residues and positions are denoted. Extensive *rfa2* N-terminal mutants (denoted by the subscript *x*) are shown as serine/threonine (S/T) residues mutated to aspartic acids (D) to mimic hyperphosphorylation or to alanines (A) to generate a nonphosphorylatable N-terminus. The extensive deletion (Δ*N*) mutant (denoted by the subscript *x*) removes amino acids 3–37. The *rfa1-t11* allele used is shown above DBD-F in Rfa1, and its amino acid change (lysine → glutamic acid; K45E) is denoted in parentheses. (C) DNA-damage assay of the *rfa2*-extensive mutants. The assay was performed exactly as described in Figure 1B. Sensitivities to increasing concentrations of phleomycin (PHL) and CPT are shown. Sensitivities to HU and MMS are shown in Figure S1.

(Thermo Scientific). Signal on the blot was detected using either myECL Imager (Thermo Scientific) or a Storm 865 (GE Healthcare).

To detect Rfa2, and its post-translational modification, 10 μl of extract was loaded onto a 8% polyacrylamide (29:1 mono:bis) gel with or without 25–50 μM Phos-Tag (Kinoshita *et al.* 2006). The gel was transferred, and the blot was blocked as previously described. The blot was incubated with rabbit polyclonal anti-Rfa2 (kindly provided by Steve Brill) at a 1:20,000 dilution in 10% skim milk for 16–20 hr. Secondary antibody incubation, washes, and developing of the blot were as described previously for Rad53. Detection of Rfa1, and its post-translational modification, was as described for Rfa2, except that 0.5 μl (out of 100 μl) protein extract was used, and the primary antibody used was rabbit anti-Rfa1 (kindly provided by Steve Brill) at a 1:40,000 dilution in 10% skim milk for 16–20 hr. All secondary antibody incubations, washes, and developing of the blot were as described for Rad53.

Measuring checkpoint adaptation

The yeast strain JKM179, containing a deletion of both *HML* and *HMR*, was used to measure the ability of cells to override G2/M arrest in the presence of DNA damage (*i.e.*, adaptation) as described previously (Lee *et al.* 1998). Two-step gene replacement was used to introduce allelic forms of *RFA1* and/or *RFA2*, as described in the strains and plasmids section. The cells were grown overnight in YPR (1% yeast extract, 2% peptone, 2% raffinose) media and single unbudded G1 cells were microdissected onto synthetic complete plates containing 2% galactose and all required amino acids (SG–Com). At 0, 8, and 24 hr, each dissected cell was examined for progression through the cell cycle as evidenced by the appearance of multiple cells (*i.e.*, cell division). Additionally, *RFA1* and *RFA2* mutant alleles were combined with other gene deletion mutations (*i.e.*, *yku70*Δ) and examined for cell division.

To measure Rad53 phosphorylation, JKM179 derivatives were grown overnight in YPD to exponential phase. These cells were then transferred to YPR and grown 12–16 hr to exponential phase (~1×10^7 cells/ml). Galactose was added to a final concentration of 2% to induce HO endonuclease expression, and cells were collected at various times after galactose addition. Protein was isolated using the method of Pellicioli *et al.* (2001). Forty micrograms of each protein sample was separated on a 7.5% (37.5:1) SDS–polyacrylamide gel, and Rad53 immunoblotting was performed as described above.

Results

Yeast RFA double mutants lacking both characterized Mec1 target sites do not display sensitivity to DNA-damaging agents

The two major *Saccharomyces* RFA phosphorylation target sites (Rfa1–S178 and Rfa2–S122) lie in the Rfa1 linker region

just upstream of DNA binding domain A (DBD-A) and in the Rfa2 loop 3–4 region (Brush *et al.* 1996; Brush and Kelly 2000; Figure 1A). Upon DNA damage, both sites (which are present as SQ motifs) are phosphorylated by the checkpoint kinase Mec1. Previous studies reported no obvious DNA-damage sensitivity when either site was mutated individually (Brush *et al.* 1996; Brush and Kelly 2000; Mallory *et al.* 2003), and in meiosis, the only detectable effect is on crossover *vs.* noncrossover frequency when Rfa2–S122 was mutated (Bartrand *et al.* 2006). Potential redundancy of these two Mec1 target sites had not been examined.

Using a genetic approach, aspartic acid (*i.e.*, phosphomimetic) or alanine (*i.e.*, nonphosphorylatable) forms of yeast Rfa1–S178 and Rfa2–S122 were generated. All possible mutant combinations were recovered by plasmid shuffle, indicating that mutation of either or both sites does not affect cell viability. When exposed to the DNA-damaging agents HU, MMS, or CPT at concentrations that cause severe lethality in an *rfa1-t11* mutant, both single mutants in either phospho-mutant form did not display damage sensitivity (Figure 1B). To rule out the possibility of redundancy (*i.e.*, phosphorylation at one site substituting for lack of phosphorylation at the other), we examined every possible double-mutant combination. None of the mutant combinations displayed sensitivity to DNA-damaging agents (Figure 1C). This indicates that although both sites are known targets for checkpoint kinase (Mec1) phosphorylation in response to damage, neither of these sites is important for the DNA-damage response.

rfa2 "extensive" mutants are viable and display sensitivity to DNA-damaging agents

The human RPA2 NT is phosphorylated in response to DNA damage. An amino-acid sequence alignment of the *S. cerevisiae* Rfa2 (NP_014087.1) and the human RPA2 (NP_002937.1) N termini revealed two prominent features (Figure 2A). First, the budding yeast Rfa2 NT is S/T rich, similar to the human RPA2 NT. Second, although there are no SQ motifs in the yeast Rfa2 NT, the number and position of S/T residues are similar to the human RPA2 NT. Phosphorylation of the yeast Rfa2 NT has been identified only in a *set1*Δ mutant during mitosis (Schramke *et al.* 2001) or by the meiosis-specific kinase Ime2 at serine 27 during meiosis (Clifford *et al.* 2004). Rad53-dependent phosphorylation of the Rfa2 NT in a *set1*Δ mutant or deletion of the Rfa2 NT (*rfa2*–Δ*40*) suppresses the MMS sensitivity of *mec3*Δ cells and results in increased expression of DNA repair genes (Schramke *et al.* 2001). Deletion of the yeast Rfa2 NT also results in shortening of telomeres (Schramke *et al.* 2004). To examine the potential physiological role of the yeast Rfa2 NT in response to DNA damage and outside of the context of a *set1*Δ or *mec3*Δ background, we generated yeast *rfa2* phospho-mutant alleles, similar to those used in many human RPA2 studies (Figure 2B).

Introduction of any Rfa2 N-terminal mutation by plasmid shuffle resulted in the formation of viable cells (Figure S1A), as indicated by growth on 5-FOA. To determine if *rfa2* phospho-mutants displayed general growth defects, the growth rate of each mutant was determined. Both the *rfa2*-D_x mutant (henceforth, subscript *x* indicates extensive mutation of all N-terminal serines/threonines; *D* indicates mutation to aspartic acids) and the *rfa2*-ΔN_x mutant (ΔN_x indicates deletion of N-terminal amino acids 3–37; similar to *rfa2*-Δ*40* in Schramke *et al.* 2001, 2004) display reduced growth when the mutant form is expressed as the only copy of *RFA2* from either from a plasmid (Table 1; RMY122-A background) or from its native chromosomal location (Table 1; JKM179 background). The reduced growth rate in the *rfa2*-ΔN_x mutant is consistent with the delayed replication observed for *rfa2*-Δ*40* (Schramke *et al.* 2001). The *rfa2*-A_x mutant (A_x indicates alanines substituted for all N-terminal serines/threonines) grew similarly to wild-type (WT) cells in either background (Table 1). This suggests that an Rfa2 NT that is either lacking or constitutively mimics phosphorylation (*i.e.*, negatively charged) results in a slight-to-modest growth defect, whereas a nonphosphorylatable Rfa2 NT mutant results in cells that grow as well as WT cells.

Table 1 Growth characteristics of *rfa2*$_x$ mutants

RFA2 allele	Strain background[a]	Growth rate (min/gen)
WT	RMY122-A	105.6 ± 11.9
rfa1-t11	RMY122-A	161.9 ± 16.6
rfa2-D_x	RMY122-A	112.1 ± 6.0
rfa2-A_x	RMY122-A	102.4 ± 4.7
rfa2-ΔN_x	RMY122-A	111.5 ± 6.0
WT	JKM179	105.6 ± 10.9
rfa1-t11	JKM179	136.1 ± 21.6
rfa2-D_x	JKM179	131.3 ± 13.9
rfa2-A_x	JKM179	108.7 ± 13.7
rfa2-ΔN_x	JKM179	144.2 ± 22.1

[a] In the strain RMY122-A, the WT or mutant *rfa2* allele is expressed from its native promoter on a low-copy centromeric vector. In the JKM179 background, the WT or mutant *rfa2* allele was integrated into its normal chromosomal location via two-step gene replacement.

rfa2 mutants were examined for sensitivity to chemical DNA-damaging agents (*e.g.*, MMS, CPT, HU, or PHL), and although each of these chemicals induces DNA damage through a different mechanism, the results were similar for each treatment. The *rfa2*-A_x mutant showed nearly indistinguishable growth compared to WT *RFA2*-containing cells on all DNA-damage-inducing media (Figure 2C, Figure S1B)—slight differences were observed only at concentrations of agents that were at least 5- to 25-fold higher than commonly used concentrations. The *rfa2*-D_x and *rfa2*-ΔN_x mutants were sensitive to all DNA-damaging agents tested (Figure 2C, Figure S1B, Figure S2).

DNA-damage sensitivity is observed only when multiple serine/threonine residues in the Rfa2 N-terminus are mutated

It is clear that *rfa2* extensive N-terminal mutants in which all of the S/T residues are mutated or deleted display damage-sensitive phenotypes. To determine which specific residue (s) might be important for the DNA-damage response, we employed a mutagenesis strategy in which single residues

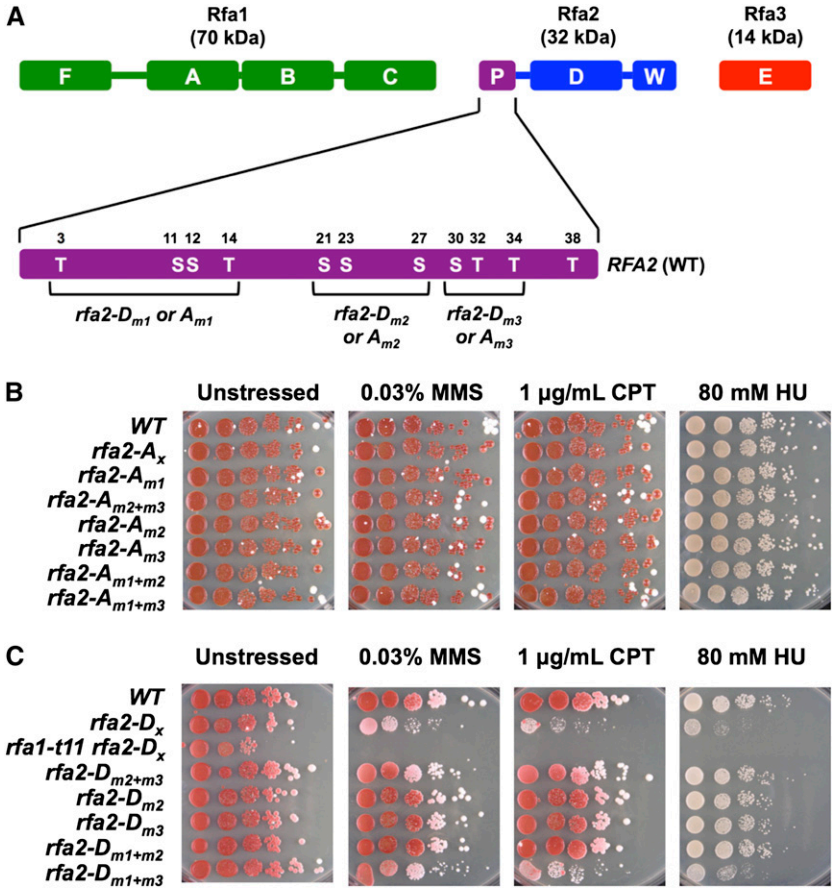

Figure 3 Phenotypic analysis of *rfa2* "multi" (*rfa2*$_m$) mutants. (A) Schematic depicting *rfa2* multimutants examined and the locations of the amino acid substitutions. Brackets indicate the clusters of serine/threonine (S/T) residues mutated to either aspartic acids, D, or alanines, A. (B) DNA-damage assays for *rfa2*-A_m mutants. *rfa2*-A_m mutants were recovered by plasmid shuffle (Figure S2A) and assayed for sensitivity to DNA damage as described in Figure 1B. (C) DNA-damage assays for *rfa2*-D_m mutants. *rfa2*-D_m mutants (Figure S2B) that could be recovered by plasmid shuffle were assayed for DNA-damage sensitivity as described in Figure 1B. *rfa2*-D_{m1} (not shown) was recovered and did not display a damage phenotype.

(individual mutants) or clusters of residues were mutated (multimutants). Shuffling-in of any *rfa2*-A_i or *rfa2*-D_i (subscript i denotes an *i*ndividual amino acid change) mutant plasmids resulted in no discernible growth phenotypes on 5-FOA, indicating that each individual mutant allele was able to complement the chromosomal *rfa2Δ* with respect to supporting normal cell growth under unstressed conditions (Figure S3A, Figure S4A). The ability to tolerate DNA damage was then examined. Although the *rfa2*-D_x mutant displayed a damage-sensitive phenotype, *rfa2*-D_i mutants were indistinguishable from WT *RFA2* cells with respect to growth on media containing DNA-damaging agents (Figure S3B). In addition, each of the *rfa2*-A_i mutants showed resistance to DNA-damaging agents similar to WT cells (Figure S4B), which was not unexpected given the lack of a DNA-damage phenotype for the *rfa2*-A_x mutant. Taken together, these results indicate that no single putative phosphorylation target site is responsible for the damage sensitivity observed for the extensive *rfa2* mutants.

The above data suggest that if N-terminal residues are physiologically important and potential targets for low-level Rfa2 phosphorylation, there might be a requirement for modification of multiple residues (*i.e.*, a critical mass of phosphorylation) to affect RFA's role in the DNA-damage response. This might also explain why single mutations have little effect, as other potential sites would remain in these mutants. To address this possibility, the Rfa2 NT was divided into three subregions, and clusters of three to four serine/threonine residues were mutated to mimic phosphorylation or to be nonphosphorylatable (Figure 3A and Table 2). These clusters are not only "geographically" partitioned, but also represent corresponding subregions of the human RPA2 NT with respect to order of phosphorylation identified by Anantha *et al.* (2007) and Liu *et al.* (2012). These multimutant alleles were also further combined to generate mutations of six to seven residues within the N-terminal region. All combinations of *rfa2*-A_m or *rfa2*-D_m multimutants supported cell growth in the absence of the original plasmid (Figure S5), and none of the alanine multimutants demonstrated a damage-sensitive phenotype (Figure 3B). DNA-damage sensitivity was observed for one aspartic acid multimutant (*rfa2*-D_{m1+m3}; Figure 3C), suggesting that mimicking constitutive phosphorylation of S/T residues in subregions 1 and 3 is responsible for some of the damage sensitivity observed for *rfa2*-D_x.

Genetic interactions with another RPA subunit mutant or with a DSB repair mutant reveal differences in rfa2 damage-sensitive mutants

Synthetic genetic interactions and epistasis studies are useful for identifying factors that act in the same pathway and/or the same complex. To identify the importance of the Rfa2 NT in a complex or pathway, we assayed for synthetic genetic interactions between *rfa2* N-terminal mutants and

Table 2 Rfa2 N-terminal regions, multimutant alleles examined, serine/threonine residues mutated, and their putative analogous residues in human RPA2

Rfa2 N-terminal region	Allele[a]	Rfa2 residues changed/removed	Putative analogous human RPA2 residues
1 (aa 3–14)	*rfa2-D*$_{m1}$, *A*$_{m1}$, or Δ*N*$_1$	T3, S11–12, T14	S4, S8, S11–13
2 (aa 21–27)	*rfa2-D*$_{m2}$, *A*$_{m2}$, or Δ*N*$_2$	S21, S23, S27	T21, S23, S29
3 (aa 30–40)	*rfa2-D*$_{m3}$, *A*$_{m3}$, or Δ*N*$_3$	S30, T32, T34	S33

[a] Multimutant allelic forms were also combined to form multimutants in which 6-7 serine/threonine (S/T) residues were mutated (*e.g.*, *rfa2-D*$_{m1+m2}$ designates a form where both regions 1 and 2 were mutated to aspartic acids (D)).

either *rfa1-t11* or *mre11*Δ, both of which individually lead to DNA-damage-sensitive phenotypes. Mre11 is a subunit of the yeast MRX complex (MRN in human cells) necessary for DSB repair and checkpoint function (Williams *et al.* 2007; Iijima *et al.* 2008; Rupnik *et al.* 2010). Synthetic genetic interaction between *rfa2* N-terminal alleles and *mre11*Δ was examined, because human RPA2 and Mre11 physically interact with one another, and this interaction appears to be regulated by the N-terminal state of human RPA2 and the N-terminus of RPA1 (Oakley *et al.* 2009). Synthetic genetic interaction with the *rfa1-t11* allele was examined, because it lies in a gene that encodes a different subunit within the same complex as Rfa2.

Genetic interactions between *rfa1-t11* and *rfa2* extensive mutants were examined by plasmid shuffle. Both the *rfa1-t11 rfa2-D*$_x$ and *rfa1-t11 rfa2-A*$_x$ double mutants were viable. However, the *rfa1-t11 rfa2-*Δ*N*$_x$ double mutant displayed synthetically lethality, as only a few 5-FOA-resistant microcolonies were observed for this mutant (Figure 4B), which were unable to be propagated any further. Thus, although both *rfa2-D*$_x$ and *rfa2-*Δ*N*$_x$ single mutants display damage-sensitive phenotypes, they display differential genetic interactions with *rfa1-t11*.

Partial deletions of the Rfa2 NT were constructed to identify which mutated subregion(s) was responsible for the DNA-damage-sensitive and/or *rfa1-t11* synthetic lethal phenotypes. Similar to the multimutants, we divided the putative phosphorylation sites into three clusters (subregions) and deleted each subregion (Figure 4A). Deletion of any cluster of putative sites did not affect the ability to shuffle out the WT *RFA2* plasmid (Figure 4B); however, DNA-damage assays revealed that *rfa2-*Δ*N*$_3$ displayed a moderate damage-sensitive phenotype, indicating that this subregion (or perhaps this cluster of S/T residues) is important in the damage response (Figure 4C). Double mutants of these partial deletion alleles and *rfa1-t11* revealed that all of the double mutants are viable, although both *rfa1-t11 rfa2-*Δ*N*$_1$ and *rfa1-t11 rfa2-*Δ*N*$_3$ display synthetic sickness, as indicated by less efficient loss of the WT *RFA2*-containing plasmid (Figure 4D) and by reduced growth of the recovered mutant on YPD under unstressed conditions (Figure 4E). Damage-sensitivity effects could not be determined in mutants containing *rfa1-t11*, as this mutation already leads to very severe damage-dependent phenotypes. It is of interest to note that *rfa2-*Δ*N*$_1$ and *rfa2-*Δ*N*$_3$ remove the same subregions that, when mutated to aspartic acids in the *rfa2-D*$_{m1+m3}$ mutant lead to a damage-sensitive phenotype (see results above and Figure 3C), suggesting that these subregions of the Rfa2 NT are important for Rfa2 function.

Although RPA and Mre11 physically interact, it has been previously demonstrated that yeast *rfa1-DAmP* (*d*ecreased *a*bundance of *m*RNA *p*erturbation) *mre11*Δ or *rfa2-DAmP mre11*Δ double mutants display a synthetic lethality phenotype (Collins *et al.* 2007), suggesting that yeast RFA and Mre11 have synergistic, yet independent, functions. It was possible that if the Rfa2 NT were important for function in the DNA-damage response, that mutation of this domain alone might account for this synthetic genetic interaction observed previously. Each of the *rfa2* N-terminal extensive mutants or *rfa1-t11* was introduced into an isogenic *mre11*Δ strain, and viability was assessed via the plasmid shuffle assay. Three interesting results were observed. First, the *rfa1-t11 mre11*Δ double mutant was synthetically lethal under unstressed conditions (Figure 5A). It was known previously that a human RPA1-t11 mutation disrupts interaction with Mre11 (Oakley *et al.* 2009); however, it is clear that the synthetic lethality observed for the *rfa1-t11 mre11*Δ double mutant in yeast is not due to lack of interaction (*i.e.*, any interaction would already be disrupted by virtue of the absence of Mre11). The data are consistent with a role for RFA independent from its interaction with Mre11. Second, the *rfa2-D*$_x$ *mre11*Δ double mutant is synthetically lethal (Figure 5A), similar to that of an *rfa1-t11 mre11*Δ double mutant. This would suggest that *rfa2-D*$_x$ and *rfa1-t11* mutants might have a fundamentally similar defect in function. Third, the *rfa2-*Δ*N*$_x$ *mre11*Δ double mutant is viable (Figure 5A), unlike the *rfa1-t11 mre11*Δ or *rfa2-D*$_x$ *mre11*Δ double mutants. This would again suggest that the defect in function in *rfa2-*Δ*N*$_x$ cells is different from that of *rfa2-D*$_x$ or *rfa1-t11*.

Since *rfa2-D*$_x$ showed a genetic interaction with *mre11*Δ, *rfa2* multimutants were utilized in an attempt to identify the subregion(s) contributing to the synthetic lethality observed in Figure 5A. *mre11*Δ *rfa2-D*$_m$ double-mutant combinations were generated and assessed for viability. Interestingly, *mre11*Δ *rfa2-D*$_{m1+m3}$ was synthetically lethal, similar to the *mre11*Δ *rfa2-D*$_x$ mutant (Figure 5B). This suggests that S21, S23, and S27 do not contribute to the genetic interaction observed for the *mre11*Δ *rfa2-D*$_x$ mutant. This is also consistent with the *rfa2-D*$_{m1+m3}$ mutant displaying the most severe damage-sensitive phenotype (Figure 3C). Finally, the double mutants *mre11*Δ *rfa2-D*$_{m2+m3}$ and *mre11*Δ *rfa2-D*$_{m3}$ show similar synthetic sickness (Figure 5, B and C). Both of

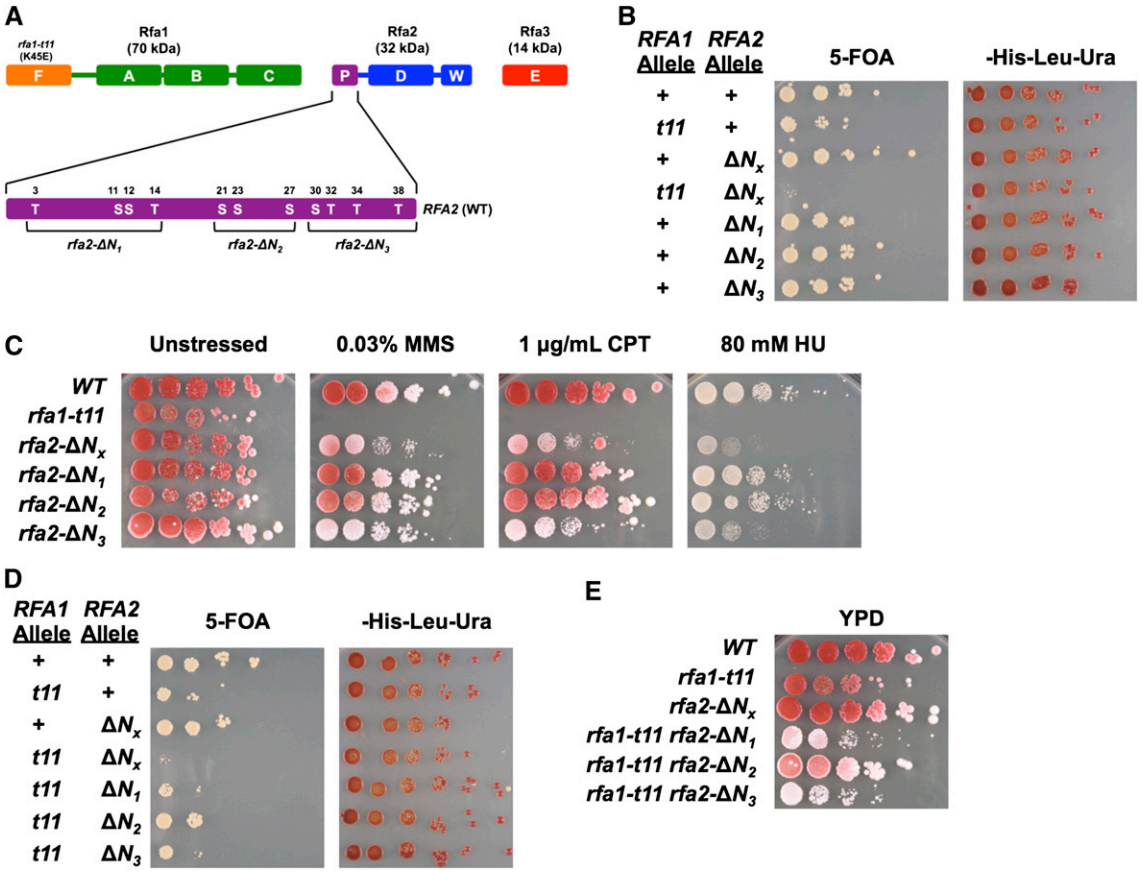

Figure 4 Genetic interactions with *rfa1-t11*. (A) Schematic of rfa2 subregion deletion mutants examined. (B) Spot assay measuring genetic interaction between *rfa2* mutants and *rfa1-t11* by plasmid shuffle. RMY122-A strains containing pJM132 were cotransformed with plasmids containing either *RFA1* or *rfa1-t11* and *rfa2* mutant alleles. Transformants were selected for on SD–His–Leu–Ura plates and "shuffling out" of pJM132 (*i.e.*, the ability of a particular mutant to support viability) was detected as growth on 5-FOA. (C) Examining which subregion of the Rfa2 N-terminus is responsible for the DNA-damage phenotypes of *rfa2*-ΔN_x strains. Damage assays for *rfa2*-ΔN_1, *rfa2*-ΔN_2, or *rfa2*-ΔN_3 strains were performed as described in Figure 1B. (D) Examining genetic interactions between *rfa2*-Δ*N* subregion mutants and *rfa1-t11*. Since *rfa2*-ΔN_x displays damage sensitivities and synthetic lethality with *rfa1-t11*, we examined *rfa2*-ΔN_1, *rfa2*-ΔN_2, or *rfa2*-ΔN_3 subregion mutants in combination with *rfa1-t11*. Cells were examined as in Figure 4B. (E) Growth assay of *rfa1-t11 rfa2*-Δ*N* subregion double mutants recovered from plasmid shuffle. Cells were grown overnight, sonicated, counted, diluted to 2.4×10^5 cells/ml, and serial diluted as threefold dilutions. The serial dilutions were spotted and examined as described in Figure 1B (damage assays are not shown, as *rfa1-t11* cells have a severe sensitivity that appears to be epistatic to any *rfa2* extensive mutant form).

these double mutants have subregion 3 mutated to aspartic acids, identifying this subregion as contributing to synthetic sickness (*i.e.*, slow growth or inviability) in an *mre11*Δ strain, when in a constitutively phosphomimetic state.

Protein phosphorylation and checkpoint initiation occurs in rfa2 N-terminal mutants in response to DNA damage

While Rfa2 is phosphorylated on S122 by Mec1 in response to DNA damage (Brush *et al.* 1996; Mallory *et al.* 2003; Bartrand *et al.* 2006), it has not been directly demonstrated that phosphorylation occurs in mitotically damaged cells in the N-terminal region of yeast Rfa2 (in a *SET1* strain). This is in stark contrast to human RPA2, where upon DNA damage, the N-terminus is hyperphosphorylated on multiple residues by ATR, ATM, and DNA-PK, displaying obvious shifts in mobility by SDS–PAGE (Liu *et al.* 2012). To determine whether the Rfa2 NT is also phosphorylated in response to DNA damage, we examined asynchronous exponentially growing cells that were either unstressed or treated with MMS, leading to replicative stress and DNA breaks. In gels containing 50 µM Phos-Tag (Kinoshita *et al.* 2006), a distinct phosphospecies was observed for all *rfa2*-extensive mutants in both exponentially growing and damaged cells (Figure 6A), similar to that observed previously (Schramke *et al.* 2001). The most important feature to note is that the shifted Rfa2 phosphospecies was present in all *rfa2*-extensive mutant cells examined, including the *rfa2*-A_x mutant lacking all S/T residues in the N-terminus, indicating that the Rfa2 NT is not a predominant target for phosphorylation.

Interestingly, we were able to observe a distinct phosphospecies using 25 µM Phos-Tag technology for the *rfa2*-D_x and *rfa2*-ΔN_x mutants. This Rfa2 species was also observed in a 50 µM Phos-Tag gel as a more diffuse and slightly higher-shifted species identified from *rfa2*-D_x mutant cells

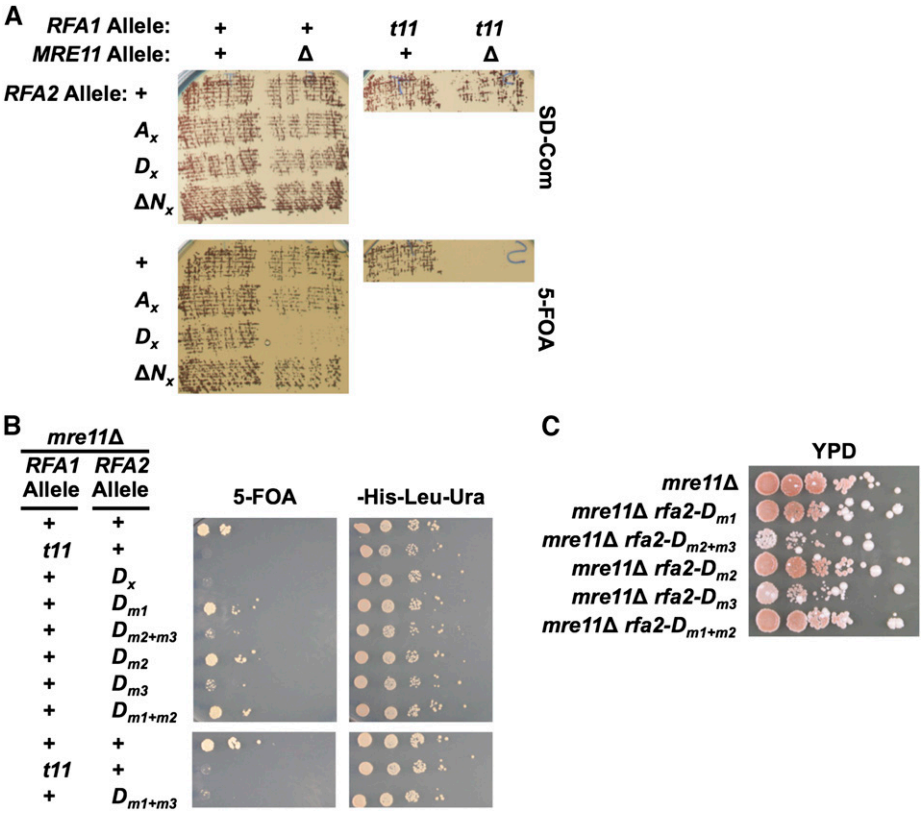

Figure 5 Genetic interactions with *mre11*Δ. (A) Replica plating to measure genetic interaction between *rfa1* or *rfa2* mutants and *mre11*Δ by plasmid shuffle. RMY122-A–*mre11*Δ strains containing pJM132 were cotransformed with plasmids containing various allele combinations of *RFA1* and *RFA2*. Transformants were selected for on SD–His–Leu–Ura plates and picked to a SD–His–Leu–Ura master plate (four independent colonies for each shuffle). "Shuffling out" of pJM132 was examined by replica plating the master plate onto SD-Com (synthetic complete with amino acids supplemented) and 5-FOA plates, and the plates were incubated at 30° for 2–4 days. Growth on 5-FOA indicates that the combination of mutant *RFA1* and/or *RFA2* alleles supports cell viability. (B) Examining which aspartic acid mutations in the Rfa2 N-terminus are responsible for the phenotype of rfa2-D_x strains. Since rfa2-D_x displays damage sensitivities and synthetic lethality with mre11Δ, we examined rfa2-D_m mutations (where the multimutant form is indicated by the subregion of the Rfa2 N-terminus as shown in Figure 3A) in combination with mre11Δ. Cells were examined as in Figure 4B. (C) Spotting of serial dilutions of *rfa2*-D_m *mre11*Δ cells recovered by plasmid shuffle. Cells were grown overnight, sonicated, counted, diluted to 2.4 × 10^5 cells/ml, and serial diluted as threefold dilutions. Five microliters of each dilution were spotted onto YPD (damage assays are not shown, as *mre11*Δ cells have a severe sensitivity that appears to be epistatic to any *rfa2* extensive mutant form).

following DNA damage, consistent with the 25 μM Phos-Tag result. This species was not present in WT, *rfa1-t11*, or *rfa2-*A_x cells. It is worth noting that this phosphospecies was observed only in *rfa2*-extensive mutants that are DNA-damage sensitive, and the species was DNA-damage specific (Figure 6A). It has not been determined if this phosphospecies is the same in *rfa2-*D_x and *rfa2-*ΔN_x cells, nor if this phosphorylation is causative of or simply correlative with DNA-damage sensitivity. Post-translational modification of Rfa1 is unaffected in all of the *rfa2*-extensive mutant cells both before and after DNA damage (Figure 6B). Although the intensity of the Rfa2 protein signal in *rfa2-*ΔN_x cells was consistently reduced, it was unclear if this is due to instability of Rfa2 protein, epitope masking, or a reduction in available epitope due to the missing N-terminus. Consistent with the latter possibilities, the level of Rfa1 protein detected is similar in all mutants (Figure 6B). Since human RPA1 stability is dependent on RPA2 (Haring *et al.* 2010), one would predict that if yeast Rfa2 were reduced, a similar reduction in Rfa1 might also occur. However, this was not observed.

One mechanism by which a mutant could display DNA-damage sensitivity is through the inability to activate, maintain, or recover properly from a checkpoint. Since human RPA2 is phosphorylated by checkpoint kinases in response to DNA damage, we surmised that the damage sensitivity observed in *rfa2* mutant yeast strains might be due to misregulation of checkpoint function. We examined G2/M checkpoint activation in *rfa2* mutants by measuring the phosphorylation of yeast Rad53 (homolog of human Chk2). Rad53 lies downstream of yeast RFA in the checkpoint pathway and becomes phosphorylated (activated) in response to DNA damage (Lee *et al.* 2000; Pellicioli and Foiani 2005; Harrison and Haber 2006; Branzei and Foiani 2006). Rad53 is phosphorylated not only in WT cells, but also in all of the *rfa2*-extensive mutants when cells are treated with MMS (Figure 6B) or when a single DSB is induced (Figure 7B). This indicates that the modification or loss of the Rfa2 NT has no observable effect on Rad53 activation and suggests that checkpoint establishment after DNA stress is unaffected.

Checkpoint adaptation in rfa2-extensive mutant strains

Checkpoint adaptation is the ability of a cell to override G2/M checkpoint arrest and proceed through the cell cycle even in the presence of unrepaired DNA damage, and it has been suggested that this is a mechanism by which cells might survive, even when damage persists (Galgoczy and Toczyski 2001). The initial phosphorylation of Rad53 is necessary to establish a checkpoint in yeast, and it should be noted that *rfa1-t11* cells have initial Rad53 phosphorylation that is indistinguishable from WT cells in response to DNA damage (Lee *et al.* 2000; Figure 6B). However, *rfa1-t11* promotes adaptation in normally adaptation-deficient *yku70*Δ or *tid1*Δ mutants that is mediated through a reduction in phosphorylation of Rad53 (Lee *et al.* 1998; Pellicioli *et al.* 2001).

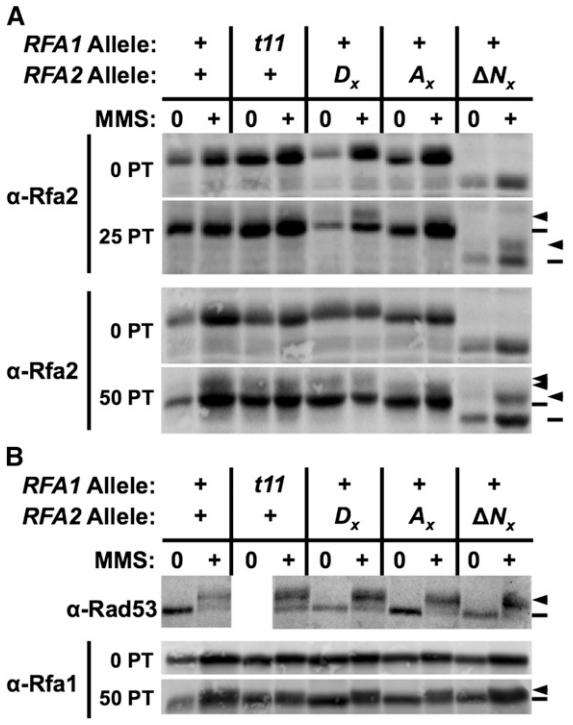

Figure 6 Phosphorylation phenotypes of *rfa2* extensive mutants. (A) Phosphorylation of Rfa2 before and after DNA damage. Cells were grown to ~1 × 10^7 cells/ml, split into two cultures, and one of the cultures was treated with 0.03% MMS for 3 hr. Following treatment, ~2 × 10^7 cells were collected and lysed, and one-tenth of each protein extract (equivalent to ~2 × 10^6 cells) was resolved in 8% polyacrylamide (29:1 mono:bis) gel in the absence or presence of Phos-Tag (PT; micromolar is indicated to left of each blot) in the gel. *RFA1* and *RFA2* alleles present and type of damage treatment is denoted above each blot. Following transfer, Rfa2 protein species were detected with rabbit polyclonal antibody to Rfa2. Dash, unphosphorylated species; arrowhead, phosphorylated/slower mobility species. Rightmost symbols represent Rfa2 species from the *rfa2*-ΔN_x strain. In gels where no Phos-Tag was added, phosphorylated/changed species were difficult to resolve. Also, note two diffuse shifted Rfa2 species from the *rfa2*-D_x strain, consistent with the shift observed for 25 mM PT. (B) Detection of Rad53 and Rfa1 proteins and post-translational modifications. For Rad53, one-tenth of the protein extract was separated in a 6% polyacrylamide (37.5:1 mono:bis) gel. For Rfa1, one-twentieth of each protein extract (equivalent to ~1 × 10^6 cells) was resolved in a 6% polyacrylamide (29:1 mono:bis) gel in the absence or presence of Phos-Tag in the gel. Proteins were detected with rabbit polyclonal antibodies to Rad53 and Rfa1, respectively. Designations are as in Figure 6A.

We have demonstrated in this study that *rfa1-t11* and *rfa2*-D_x mutants both displayed damage sensitivity, and each displayed synthetic lethality when combined with *mre11*Δ. We addressed whether *rfa2* N-terminal mutants affect adaptation. In the presence of a single, irreparable DSB at the *MAT* locus, *rfa2*-D_x or *rfa2*-A_x mutant cells are capable of arresting at the G2/M checkpoint by 8 hr similar to WT cells, as indicated microscopically as a cell with a single large bud (Figure 7A) and by phosphorylation (activation) of Rad53 (Figure 7C). However, only *rfa2*-D_x cells display an adaptation frequency that is nearly indistinguishable from WT or *rfa1-t11* cells (Figure 7B). Furthermore, when *rfa2*-D_x was combined with *yku70*Δ (normally adaptation deficient), the cells now showed adaptation proficiency, similar to that reported previously for *rfa1-t11 yku70*Δ cells (Lee *et al.* 1998; Figure 7, A and B). This is corroborated by the observation that the majority of Rad53 is not phosphorylated by 18 hr after induction of a DSB (Figure 7D) in these cells.

Interestingly, *rfa2*-A_x cells display reduced adaptation (Figure 7, A and B) and a slightly later reduction in phosphorylation of Rad53 after DNA damage (Figure 7C). Furthermore, the *rfa2*-A_x *yku70*Δ mutant is adaptation deficient, similar to the *yku70*Δ single mutant (Figure 7B). Supporting *rfa2*-A_x *yku70*Δ adaptation deficiency is the inability of Rad53 to be dephosphorylated, even 18 hr after damage induction (Figure 7D).

Discussion

The N-terminal region of Rfa2 is important for proper cellular response to DNA damage

The results presented in this work demonstrate that the N-terminus of yeast Rfa2 is required for a proper DNA-damage response. This is indicated by the fact that removal of this domain (*rfa2*-ΔN_x) leads to DNA-damage-sensitive phenotypes. However, phosphorylation of the yeast Rfa2 NT is not necessary for cells to respond to repairable DNA damage, since cells bearing a nonphosphorylatable form of this domain (*rfa2*-A_x) exhibit near wild-type growth and DNA-damage-tolerance phenotypes.

Using Western blotting and Phos-Tag technology, we were unable to detect major differences in yeast Rfa2 phosphorylation in the *rfa2* NT mutants, except for an additional phosphospecies in the damage-sensitive *rfa2* mutants only. The additional modification observed must reside outside of the Rfa2 NT, as it is observed in the *rfa2*-ΔN_x mutant. This indicates that the *Saccharomyces* Rfa2 NT is not the predominant region for damage-induced phosphorylation, but that the state of this domain can influence the damage response and/or additional modification of Rfa2 outside of the N-terminus. The lack of readily detectable damage-specific phosphorylation in the yeast Rfa2 NT is in stark contrast to the human RPA2 NT, but is completely consistent with the observation that *rfa2*-A_x mutant yeast cells are resistant to DNA damage.

It is worth noting that even in N-terminal mutants where DNA-damage sensitivity was observed, post-translational modification of Rfa1 did not appear to be affected. Despite the apparent lack of major phosphorylation in the WT Rfa2 NT, we note that when individual residues on RFA (Rfa1–S178 and Rfa2–S122) previously identified to be phosphorylated by Mec1 are mutated to nonphosphorylatable forms (or phosphomimetic forms), there was no observable DNA-damage-sensitive phenotype. This indicates that Rfa1–S178 and Rfa2–S122 are neither redundant nor important for the damage response or that any mutant phenotype is so subtle that it cannot be detected by the assays performed in this study. As our study was done in haploid strains growing mitotically, this does not preclude the importance of post-translational modification of these residues in meiosis, where a phenotype

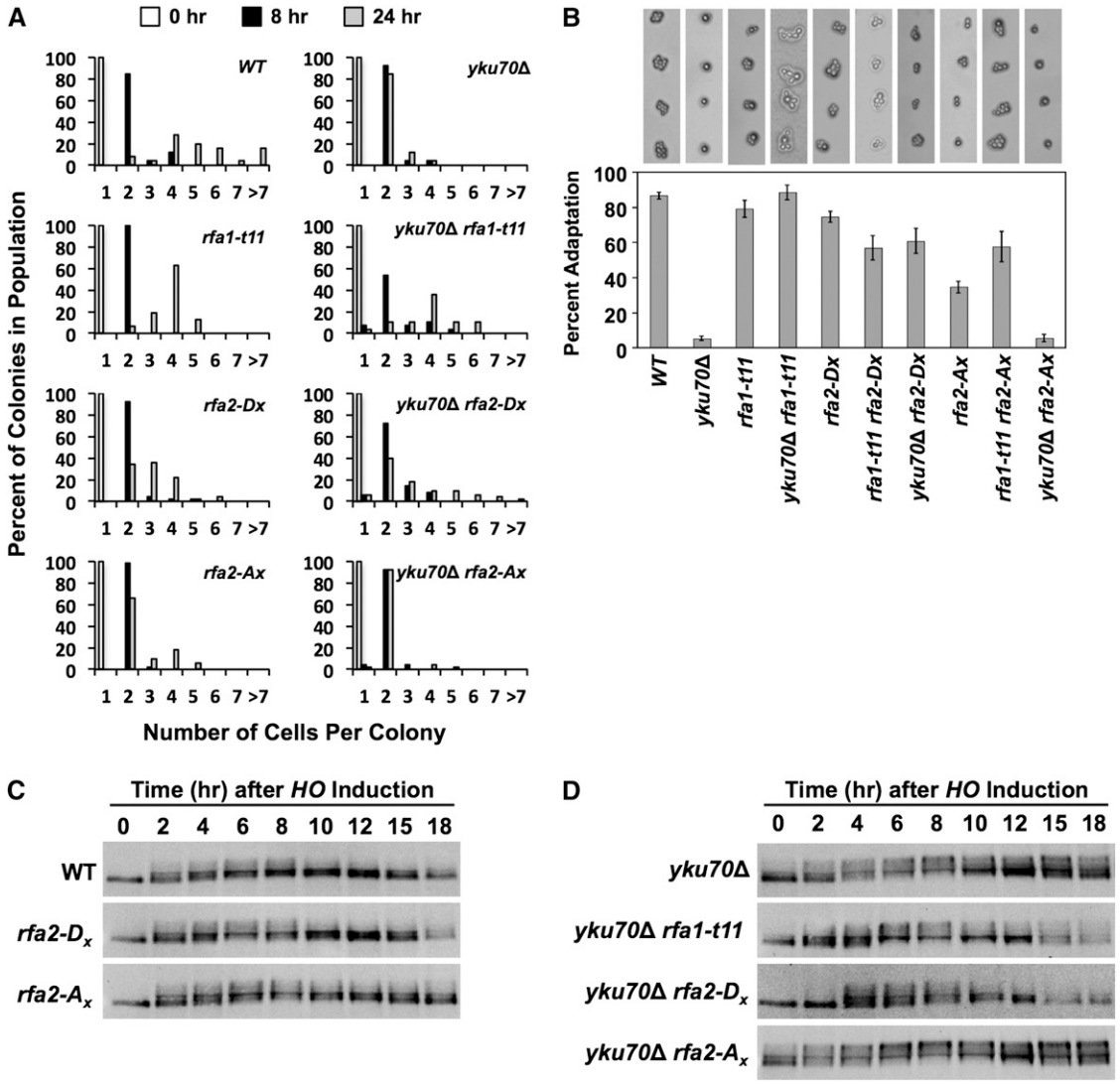

Figure 7 Checkpoint adaptation phenotypes of *rfa2* extensive mutants. (A) Adaptation phenotypes in *rfa2-D*$_x$ and *rfa2-A*$_x$ mutant cells at 0, 8, and 24 hr after HO break induction. Microdissection was used to identify and separate early S-phase cells onto SG-Com plates, which led to expression of HO endonuclease. After 0, 8, and 24 hr, cells were examined microscopically and quantitated for number of cells observed for each colony. (B) Quantitation and microscopic representation of adaptation after 24-hr post-HO break induction. Microscopic representation (top), and multiple independent experiments ($N > 8$ for all strains) were quantitated (bottom) to determine the percentage of colonies with >2 cells. (C) Rad53 phosphorylation in *rfa2*-extensive mutants. Expression of HO endonuclease was induced in exponentially growing cells by the addition of 2% galactose to the media. Cells were collected at various time points following galactose addition, and 40 μg of whole-cell extracts were probed with anti-Rad53 antibody. Slower migrating species indicate phosphorylated Rad53 (as described in Pellicioli *et al.* 2001). (D) The effect of *rfa2*-extensive mutations on Rad53 phosphorylation state in yku70Δ strains. Phosphorylation of Rad53 was examined as described in Figure 7C. *yku70*Δ and *yku70*Δ *rfa1-t11* were previously examined in Pellicioli *et al.* 2001 and are controls for Rad53 phosphorylation in adaptation-deficient and adaptation-proficient strains, respectively.

has been observed for Rfa2–S122 mutants (Bartrand *et al.* 2006). It is clear that the phenotypes observed for N-terminal mutants of yeast Rfa2 are far more severe than those for known phosphorylation target-site mutants, suggesting that similar to human RPA2, the N-terminal region is more important for the DNA-damage response.

Subregions 1 and 3 are responsible for phenotypes observed in Rfa2 N-terminal mutants

All *rfa2* individual site mutants showed robust growth and resistance to DNA damage, suggesting that perturbing one site in the Rfa2 NT is not enough to elicit a phenotype. Although we could not detect an obvious lack of phosphorylation in any of the *rfa2*-extensive mutants in response to DNA damage, we did observe that certain regions of the Rfa2 NT were more sensitive to alteration than others. Dividing the yeast Rfa2 NT into three subregions revealed that all of the growth defects, DNA-damage defects, and genetic interactions we observed could be attributed to mutation of subregion 1 (aa 3–14) and/or subregion 3 (aa 30–40) of the N-terminus (Table 3). It is interesting to note that subregions 1 and 3 are analogous to subregions of human RPA2

Table 3 Qualitative summary of *rfa2* N-terminal mutant phenotypes and genetic interactions

RFA2 allele	Mitotic growth[b]	Damage resistance[a,b]	Genetic interaction[a]		Adaptation[a]	
			rfa1-t11	*mre11*Δ	*YKU70*	*yku70*Δ
WT	+++++	+++++	NA	NA	Proficient	Deficient
rfa1-t11	+	0	NA	Lethality	Proficient	Proficient
rfa2-D$_x$	+++	++	None	Lethality	Proficient	Proficient
rfa2-A$_x$	+++++	+++++	None	None	Reduced	Deficient
*rfa2-*Δ*N*$_x$	+++	++	Lethality	None	ND	ND
rfa2-D$_{m1+m3}$	+++++	+++	ND	Lethality	ND	ND
*rfa2-*Δ*N*$_1$	+++++	++++	Sickness	ND	ND	ND
*rfa2-*Δ*N*$_3$	+++++	++	Sickness	ND	ND	ND
rfa2-D$_{m2+m3}$	+++++	++	ND	Sickness	ND	ND
rfa2-D$_{m3}$	+++++	+++++	ND	Sickness	ND	ND

[a] NA, not available/applicable; ND, not determined.
[b] Scale is +++++, best growth/most damage resistant; +++, moderate growth/moderately damage resistant; +, slow growth/slightly damage resistant; 0, no growth/not damage resistant.

(Table 3) that contain all but one (T21) of the primary DNA-damage-specific targets of checkpoint kinases (Anantha *et al.* 2007; Liu *et al.* 2012). If low-level (currently undetectable) post-translational modification is occurring in the Rfa2 NT, we would suggest that it is potentially occurring in both of these subregions. Alternatively, these subregions are important and may have evolved in higher eukaryotes to be post-translationally modified during DNA damage for reasons that are not yet clear.

Genetic interactions suggest overlapping, yet different functions for the yeast Rfa1 and Rfa2 N termini

Phosphorylation (or phosphomimetic mutations) of the human RPA2 NT can have an effect in regulating protein interactions and/or DNA interactions that involve the N-terminus of RPA1 (DBD-F). Evidence that a phosphomimetic RPA2 N-terminal peptide affects the NMR structure of purified RPA1 DBD-F in a fashion similar to that of ssDNA binding to RPA1 DBD-F suggests that this peptide competes with ssDNA for binding to DBD-F (Binz *et al.* 2003). Furthermore, it has been demonstrated that DBD-F is important for interaction of human RPA1 with human Mre11, and mutation of this domain (RPA1-t11) or a phosphomimetic form of human RPA2 (RPA2-*D*$_x$) disrupts this interaction (Oakley *et al.* 2009).

Based on this idea, one might conjecture that a yeast *rfa2-D*$_x$ mutant would behave similarly to an *rfa1-t11* mutant. In this regard, both mutants grew more slowly, displayed damage sensitivities, were synthetically lethal in combination with *mre11*Δ, and exhibited the ability to promote adaptation in a *yku70*Δ background. This is consistent with a model in which a phosphorylated RPA2 N-terminus affects the function of the RPA1 N-terminus (DBD-F), similar to if DBD-F were mutated. It has not been determined whether a phosphomimetic human RPA2 affects the NMR structure of an RPA1-t11 (DBD-F) mutant. However, our results are consistent with this model in which hyperphosphorylated yeast Rfa2 interacts with DBD-F of yeast Rfa1 to potentially disrupt protein/DNA interactions.

Despite both being DNA-damage sensitive, it is clear that the defect(s) in *rfa2-D*$_x$ mutants differs from the defect(s) in *rfa2-*Δ*N*$_x$ mutants. The *rfa2-*Δ*N*$_x$ mutant is intriguing, because it does not behave like an *rfa2-A*$_x$ mutant, even though neither of these Rfa2 proteins is phosphorylatable on their N-terminus. This clearly delineates between a requirement for the presence of the domain *vs.* a requirement for phosphorylation of the domain. Perhaps more intriguing is the fact that the *rfa2-*Δ*N*$_x$ mutant does not display a genetic interaction with *mre11*Δ, but does display a genetic interaction with *rfa1-t11*. This suggests that removal of the Rfa2 NT results in a cellular defect similar to when Mre11 is deleted. Furthermore, deletion of the Rfa2 NT confers a defect distinct from that observed in *rfa1-t11* mutant cells that lack a functional DBD-F. It has been proposed that the human RPA2 N-terminus may function by regulating the function of the human RPA1 N-terminus (Binz *et al.* 2003; Oakley *et al.* 2009). These studies indicate that the Rfa2 N-terminus has a role beyond regulating the Rfa1 N-terminus, and it will be important to determine what that role(s) is.

Transition from a "normal" damage response to adaptation may depend on the Rfa2 N-terminus

In this study, a nonphosphorylatable N-terminal form of Rfa2 functions nearly indistinguishably from WT Rfa2 after DNA damage. Perhaps more importantly, the *rfa2-D*$_x$ mutant is damage sensitive. Therefore, it is curious that in response to DNA damage, human RPA2 is hyperphosphorylated on its N-terminus. Differences between yeast Rfa2 and human RPA2 might simply be caused by cellular complexity (*e.g.*, human RPA interacts with proteins not found in yeast cells and might require additional modification to regulate these interactions). Alternatively, differences could be due to the experimental parameters of studies performed in human tissue culture *vs.* yeast. Whatever the case, it is clear that lack of phosphorylation in the Rfa2 NT is tolerated quite well under commonly used DNA-damage assay conditions in yeast.

What if the DNA lesion was such that it was either difficult to repair or, perhaps, irreparable? A feature shared

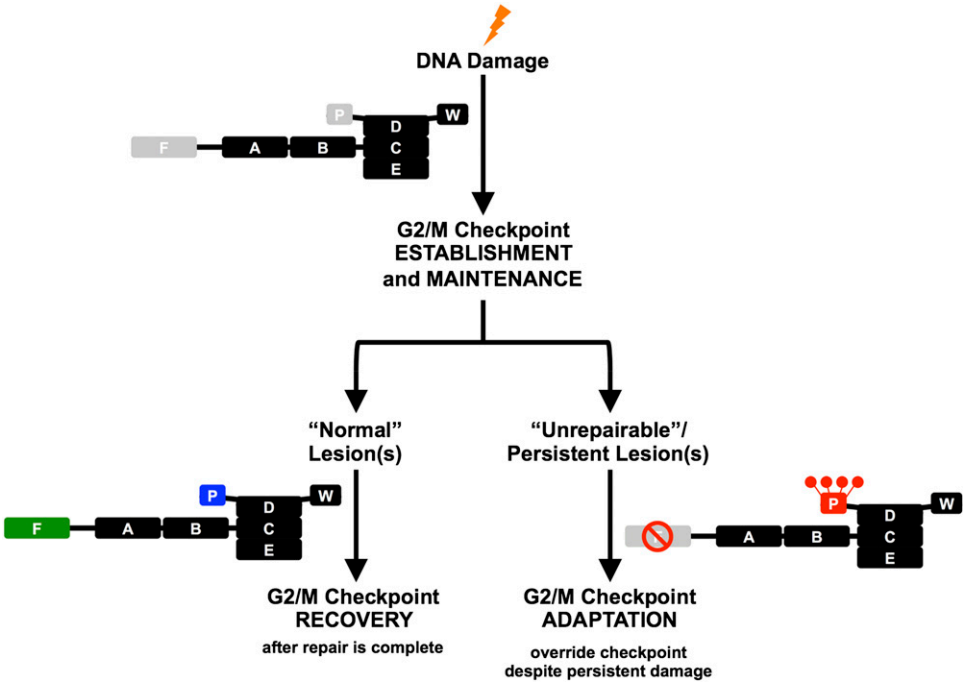

Figure 8 Model for Rfa2 N-terminus function in checkpoint maintenance and adaptation. In response to DNA damage, cells undergo recognition of the lesion and signaling to halt the cell cycle by establishing the G2/M checkpoint. The initiation of the checkpoint response occurs, regardless of the state of the N-terminus of either Rfa1 or Rfa2 (denoted as gray boxes to indicate each is either inactive or not present). The decision to override the checkpoint is affected by the state of the Rfa1 and/or Rfa2 N termini. Cells with a functional Rfa1 DBD-F (denoted by a green box) or Rfa2 where the N-terminus is present and in a nonphosphorylated state (denoted by a blue box) appear to less readily adapt, suggesting a propensity to maintain checkpoint function until repair is complete followed by proper checkpoint recovery. If damage persists, the N-terminus of Rfa1 may be inactivated (denoted by a gray box with red slashed circles) and/or the Rfa2 N-terminus may become phosphorylated (denoted by multiple red circles). The Rfa2 N-terminus may not be phosphorylated or may be dephosphorylated when normal ("repairable") DNA damage is present; however, upon persistent ("irreparable") damage, modification of the Rfa2 N-terminus may occur to promote entry into M-phase as a "last-ditch effort" for cell survival.

between a cell that is permanently arrested *vs.* a cell that is inviable is that neither is "growing." Checkpoint adaptation allows for the possibility of cell growth, with the potential for the lesion to be repaired later. Although genome stability appears to be compromised [*i.e.*, increased spontaneous chromosome loss and break-induced repair (BIR)] in adaptation-proficient mutants, it has also been demonstrated that adaptation results in cells with higher resistance upon exposure to DNA-damaging agents (*e.g.*, X irradiation) in diploid cells (Galgoczy and Toczyski 2001). It is clear that all of the *rfa2*-extensive mutants display initial phosphorylation of Rad53 indistinguishable from WT cells following MMS treatment or 8 hr after an HO-induced DSB. This would suggest that a G2/M checkpoint establishment defect is not the explanation for the damage sensitivity observed for some *rfa2* N-terminal mutants. However, we have observed that the *rfa2-D*$_x$ mutant promotes adaptation when combined with *yku70*Δ, similar to that observed for *rfa1-t11*. There is a precedent for checkpoint release in human cells, as it has been demonstrated that RPA2 N-terminal phosphorylation is necessary to exit M phase and enter G1 phase in the presence of mitotic DNA damage (Anantha *et al.* 2008). We propose that the DNA-damage sensitivity observed for *rfa2-D*$_x$ strains may indeed be due to the ability to promote premature adaptation, resulting in mitotic division despite the persistence of damaged DNA. If cells "adapt" during continued/prolonged treatment with genotoxic agents (*i.e.*, spot assays on plates containing DNA-damaging agents), the lack of arrest and coupled increase in genomic instability would presumably lead to additional DNA damage and/or chromosomal loss. Although tolerated in diploid cells (Galgoczy and Toczyski 2001), this would be quite detrimental to the haploid cells in our studies and would manifest as reduced colony growth in a damage assay. Our data corroborate the idea that adaptation is beneficial to the cell only when it has a diploid genome content to compensate for chromosomal loss or rearrangement.

It is worth noting that *rfa2-A*$_x$ mutants were indistinguishable from WT cells in almost every assay, except for adaptation. In fact, the *rfa2-A*$_x$ mutant displayed an adaptation-reduced phenotype and became fully adaptation proficient only when combined with an *rfa1-t11* mutation. This suggests that the lack of serine/threonine residues and/or an inability to post-translationally modify these residues in the Rfa2 NT inhibits adaptation in otherwise WT cells (and especially in *yku70*Δ cells). Because these cells prolong resistance to progression into M phase until DNA damage has been repaired, this is a plausible explanation for why they do not display DNA-damage sensitivities using common DNA stressors. Despite being adaptation-deficient, *rfa2-A*$_x$ cells grow indistinguishably from WT cells in the absence of stress, indicating that the inability to enter M phase is reduced only in the presence of unrepaired DNA and not under unstressed conditions.

We propose a model (Figure 8) in which the yeast Rfa2 NT plays a role in determining whether cells adapt. In this model, we propose that prolonged checkpoint arrest will lead to adaptation through "inactivation" of the yeast Rfa1 N-terminus (DBD-F; similar to that of the *rfa1-t11* mutation) or modification of the yeast Rfa2 N-terminus (Figure 8, right

side). Alternatively, an inability to disrupt Rfa1 DBD-F function or lack of modification of the Rfa2 NT in the presence of DNA damage helps to reinforce (*i.e.*, maintain) the checkpoint until the damage is repaired, promoting proper checkpoint recovery (Figure 8, left side). Consistent with this, a nonphosphorylatable *rfa2* NT mutant displays reduced adaptation. In cases where damage is repairable and adaptation would not be necessary, the *rfa2* mutants that are nonphosphorylatable (*rfa2*-A_x and *rfa2*-ΔN_x) display very different phenotypes, indicating that there is a difference between having a domain that cannot be phosphorylated on serine/threonine residues and not having the domain at all, as long as the damage is repairable and does not persist.

It is important to address the physiological importance of hyperphosphorylation of RPA2 in response to DNA damage in human (and potentially many higher eukaryotic) cells. It is also important to understand how yeast accomplish proper DNA repair and cell-cycle regulation without obvious post-translational modification of the Rfa2 NT. Why this domain is necessary in yeast, but post-translational modification is not, will be of importance in identifying the mechanism(s) of RFA function, not only in yeast, but perhaps in other eukaryotic organisms where phosphorylation of the RPA2 N-terminus is not necessary or does not occur in response to DNA damage.

Acknowledgments

We thank Steven Brill for providing antibodies to Rfa1 and Rfa2, for *RFA2* plasmids, and for the plasmid shuffle strain and Jim Haber for providing JKM179 and the *rfa1-t11* and *yku70*Δ derivatives for adaptation studies. We also thank Jodie Haring and the North Dakota State University Center for Protease Research for technical assistance. Thanks go to Julia Bowsher, Jennifer Momsen, Erika Offerdahl, and Debra Walther for insightful comments and assistance on this manuscript. This work was supported by the National Science Foundation (NSF-CAREER-1253723) and startup funds provided by North Dakota State University, the National Institute of Justice (NIJ-2004RGCX-K001), and the National Institutes of Health (NIH-P20RR015566) to S.J.H. Additional funding was provided by the Cedar Crest College (CCC) Department of Biological Sciences and the CCC Faculty Development Fund to A.P.W., the Pennsylvania Academy of Sciences Undergraduate Research Grant to S.K.K., and the American Society of Microbiology to S.J.K. and S.K.K.

Literature Cited

Albuquerque, C. P., M. B. Smolka, S. H. Payne, V. Bafna, J. Eng *et al.*, 2008 A multidimensional chromatography technology for in-depth phosphoproteome analysis. Mol. Cell. Proteomics 7: 1389–1396.

Anantha, R. W., and J. A. Borowiec, 2009 Mitotic crisis: the unmasking of a novel role for RPA. Cell Cycle 8: 357–361.

Anantha, R. W., V. M. Vassin, and J. A. Borowiec, 2007 Sequential and synergistic modification of human RPA stimulates chromosomal DNA repair. J. Biol. Chem. 282: 35910–35923.

Anantha, R. W., E. Sokolova, and J. A. Borowiec, 2008 RPA phosphorylation facilitates mitotic exit in response to mitotic DNA damage. Proc. Natl. Acad. Sci. USA 105: 12903–12908.

Ashton, N. W., E. Bolderson, L. Cubeddu, K. J. O'Byrne, and D. J. Richard, 2013 Human single-stranded DNA binding proteins are essential for maintaining genomic stability. BMC Mol. Biol. 14: 9.

Bartrand, A. J., D. Iyasu, and G. S. Brush, 2004 DNA stimulates Mec1-mediated phosphorylation of Replication Protein A. J. Biol. Chem. 279: 26762–26767.

Bartrand, A. J., D. Iyasu, S. M. Marinco, and G. S. Brush, 2006 Evidence of meiotic crossover control in *Saccharomyces cerevisiae* through Mec1-mediated phosphorylation of Replication Protein A. Genetics 172: 27–39.

Binz, S. K., Y. Lao, D. F. Lowry, and M. S. Wold, 2003 The phosphorylation domain of the 32-kDa subunit of Replication Protein A (RPA) modulates RPA–DNA interactions: evidence for an intersubunit interaction. J. Biol. Chem. 278: 35584–35591.

Branzei, D., and M. Foiani, 2006 The Rad53 signal transduction pathway: replication fork stabilization, DNA repair, and adaptation. Exp. Cell Res. 312: 2654–2659.

Brush, G. S., and T. J. Kelly, 2000 Phosphorylation of the Replication Protein A large subunit in the *Saccharomyces cerevisiae* checkpoint response. Nucleic Acids Res. 28: 3725–3732.

Brush, G. S., D. M. Morrow, P. Hieter, and T. J. Kelly, 1996 The ATM homologue MEC1 is required for phosphorylation of Replication Protein A in yeast. Proc. Natl. Acad. Sci. USA 93: 15075–15080.

Brush, G. S., D. M. Clifford, S. M. Marinco, and A. J. Bartrand, 2001 Replication protein A is sequentially phosphorylated during meiosis. Nucleic Acids Res. 29: 4808–4817.

Burgess, R. C., S. Rahman, M. Lisby, R. Rothstein, and X. Zhao, 2007 The Slx5-Slx8 complex affects sumoylation of DNA repair proteins and negatively regulates recombination. Mol. Cell. Biol. 27: 6153–6162.

Choudhary, C., C. Kumar, F. Gnad, M. L. Nielsen, M. Rehman *et al.*, 2009 Lysine acetylation targets protein complexes and co-regulates major cellular functions. Science 325: 834–840.

Clifford, D. M., S. M. Marinco, and G. S. Brush, 2004 The meiosis-specific protein kinase Ime2 directs phosphorylation of Replication Protein A. J. Biol. Chem. 279: 6163–6170.

Clifford, D. M., K. E. Stark, K. E. Gardner, S. Hoffmann-Benning, and G. S. Brush, 2005 Mechanistic insight into the Cdc28-related protein kinase Ime2 through analysis of Replication Protein A phosphorylation. Cell Cycle 4: 1826–1833.

Collins, S. R., K. M. Miller, N. L. Maas, A. Roguev, J. Fillingham *et al.*, 2007 Functional dissection of protein complexes involved in yeast chromosome biology using a genetic interaction map. Nature 446: 806–810.

Cremona, C. A., P. Sarangi, Y. Yang, L. E. Hang, S. Rahman *et al.*, 2012 Extensive DNA damage-induced sumoylation contributes to replication and repair and acts in addition to the mec1 checkpoint. Mol. Cell 45: 422–432.

Cruet-Hennequart, S., M. T. Glynn, L. S. Murillo, S. Coyne, and M. P. Carty, 2008 Enhanced DNA-PK-mediated RPA2 hyperphosphorylation in DNA polymerase eta-deficient human cells treated with cisplatin and oxaliplatin. DNA Rep. 7: 582–596.

Din, S., S. J. Brill, M. P. Fairman, and B. Stillman, 1990 Cell-cycle-regulated phosphorylation of DNA Replication Factor A from human and yeast cells. Genes Dev. 4: 968–977.

Dou, H., C. Huang, M. Singh, P. B. Carpenter, and E. T. H. Yeh, 2010 Regulation of DNA repair through deSUMOylation and SUMOylation of Replication Protein A complex. Mol. Cell 39: 333–345.

Dutta, A., S. Din, S. J. Brill, and B. Stillman, 1991 Phosphorylation of Replication Protein A: a role for cdc2 kinase in G1/S regulation. Cold Spring Harb. Symp. Quant. Biol. 56: 315–324.

Fanning, E., V. Klimovich, and A. R. Nager, 2006 A dynamic model for Replication Protein A (RPA) function in DNA processing pathways. Nucleic Acids Res. 34: 4126–4137.

Feng, J., T. Wakeman, S. Yong, X. Wu, S. Kornbluth *et al.*, 2009 Protein phosphatase 2A-dependent dephosphorylation of Replication Protein A is required for the repair of DNA breaks induced by replication stress. Mol. Cell. Biol. 29: 5696–5709.

Firmenich, A. A., M. Elias-Arnanz, and P. Berg, 1995 A novel allele of *Saccharomyces cerevisiae* RFA1 that is deficient in recombination and repair and suppressible by RAD52. Mol. Cell. Biol. 15: 1620–1631.

Flynn, R. L., and L. Zou, 2010 Oligonucleotide/oligosaccharide-binding fold proteins: a growing family of genome guardians. Crit. Rev. Biochem. Mol. Biol. 45: 266–275.

Galgoczy, D. J., and D. P. Toczyski, 2001 Checkpoint adaptation precedes spontaneous and damage-induced genomic instability in yeast. Mol. Cell. Biol. 21: 1710–1718.

Gao, J.-X., H.-T. Wang, A. H.-H. Wong, G.-S. Zeng, Z.-X. Huang *et al.*, 2014 Regulation of Rfa2 phosphorylation in response to genotoxic stress in *Candida albicans*. Mol. Microbiol. 94: 141–155.

Gnad, F., L. M. F. de Godoy, J. Cox, N. Neuhauser, S. Ren *et al.*, 2009 High-accuracy identification and bioinformatic analysis of in vivo protein phosphorylation sites in yeast. Proteomics 9: 4642–4652.

Haring, S. J., T. D. Humphreys, and M. S. Wold, 2010 A naturally occurring human RPA subunit homolog does not support DNA replication or cell-cycle progression. Nucleic Acids Res. 38: 846–858.

Harrison, J. C., and J. E. Haber, 2006 Surviving the breakup: the DNA damage checkpoint. Annu. Rev. Genet. 40: 209–235.

Helbig, A. O., S. Rosati, P. W. W. M. Pijnappel, B. van Breukelen, M. H. T. H. Timmers *et al.*, 2010 Perturbation of the yeast *N*-acetyltransferase NatB induces elevation of protein phosphorylation levels. BMC Genomics 11: 685.

Henricksen, L. A., T. Carter, A. Dutta, and M. S. Wold, 1996 Phosphorylation of human Replication Protein A by the DNA-dependent protein kinase is involved in the modulation of DNA replication. Nucleic Acids Res. 24: 3107–3112.

Holt, L. J., B. B. Tuch, J. Villen, A. D. Johnson, S. P. Gygi *et al.*, 2009 Global analysis of Cdk1 substrate phosphorylation sites provides insights into evolution. Science 325: 1682–1686.

Iftode, C., Y. Daniely, and J. A. Borowiec, 1999 Replication protein A (RPA): the eukaryotic SSB. Crit. Rev. Biochem. Mol. Biol. 34: 141–180.

Iijima, K., M. Ohara, R. Seki, and H. Tauchi, 2008 Dancing on damaged chromatin: functions of ATM and the RAD50/MRE11/NBS1 complex in cellular responses to DNA damage. J. Radiat. Res. 49: 451–464.

Kim, H.-S., and S. J. Brill, 2003 MEC1-dependent phosphorylation of yeast RPA1 in vitro. DNA Repair 2: 1321–1335.

Kinoshita, E., E. Kinoshita-Kikuta, K. Takiyama, and T. Koike, 2006 Phosphate-binding tag, a new tool to visualize phosphorylated proteins. Mol. Cell. Proteomics MCP 5: 749–757.

Kushnirov, V. V., 2000 Rapid and reliable protein extraction from yeast. Yeast 16: 857–860.

Lee, D.-H., Y. Pan, S. Kanner, P. Sung, J. A. Borowiec *et al.*, 2010 A PP4 phosphatase complex dephosphorylates RPA2 to facilitate DNA repair via homologous recombination. Nat. Struct. Mol. Biol. 17: 365–372.

Lee, S. E., J. K. Moore, A. Holmes, K. Umezu, R. D. Kolodner *et al.*, 1998 Saccharomyces Ku70, mre11/rad50 and RPA proteins regulate adaptation to G2/M arrest after DNA damage. Cell 94: 399–409.

Lee, S. E., A. Pellicioli, J. Demeter, M. P. Vaze, A. P. Gasch *et al.*, 2000 Arrest, adaptation, and recovery following a chromosome double-strand break in *Saccharomyces cerevisiae*. Cold Spring Harb. Symp. Quant. Biol. 65: 303–314.

Liaw, H., D. Lee, and K. Myung, 2011 DNA-PK-dependent RPA2 hyperphosphorylation facilitates DNA repair and suppresses sister chromatid exchange. PLoS ONE 6: 1–10.

Liu, V. F., N. V. Boubnov, and D. T. Weaver, 1995 Cell cycle checkpoints and repair of ionizing radiation damage. Stem Cells 13(Suppl. 1): 117–128.

Liu, Y., M. Kvaratskhelia, S. Hess, Y. Qu, and Y. Zou, 2005 Modulation of Replication Protein A function by its hyperphosphorylation-induced conformational change involving DNA binding domain B. J. Biol. Chem. 280: 32775–32783.

Liu, S., S. O. Opiyo, K. Manthey, J. G. Glanzer, A. K. Ashley *et al.*, 2012 Distinct roles for DNA-PK, ATM and ATR in RPA phosphorylation and checkpoint activation in response to replication stress. Nucleic Acids Res. 40: 10780–10794.

Longhese, M. P., P. Plevani, and G. Lucchini, 1994 Replication Factor A is required in vivo for DNA replication, repair, and recombination. Mol. Cell. Biol. 14: 7884–7890.

Longhese, M. P., H. Neecke, V. Paciotti, G. Lucchini, and P. Plevani, 1996 The 70 kDa subunit of Replication Protein A is required for the G1/S and intra-S DNA damage checkpoints in budding yeast. Nucleic Acids Res. 24: 3533–3537.

Mallory, J. C., V. I. Bashkirov, K. M. Trujillo, J. A. Solinger, M. Dominska *et al.*, 2003 Amino acid changes in Xrs2p, Dun1p, and Rfa2p that remove the preferred targets of the ATM family of protein kinases do not affect DNA repair or telomere length in *Saccharomyces cerevisiae*. DNA Repair 2: 1041–1064.

Maniar, H. S., R. Wilson, and S. J. Brill, 1997 Roles of Replication Protein-A subunits 2 and 3 in DNA replication fork movement in *Saccharomyces cerevisiae*. Genetics 145: 891–902.

Mimitou, E. P., and L. S. Symington, 2011 DNA end resection: unraveling the tail. DNA Repair 10: 344–348.

Oakley, G. G., and S. M. Patrick, 2010 Replication Protein A: Directing Traffic at the Intersection of Replication and Repair. Front. Biosci. (Landmark Ed.) 15:883–900.

Oakley, G. G., S. M. Patrick, J. Yao, M. P. Carty, J. J. Turchi *et al.*, 2003 RPA phosphorylation in mitosis alters DNA binding and protein-protein interactions. Biochemistry 42: 3255–3264.

Oakley, G. G., K. Tillison, S. A. Opiyo, J. G. Glanzer, J. M. Horn *et al.*, 2009 Physical interaction between Replication Protein A (RPA) and MRN: involvement of RPA2 phosphorylation and the N-terminus of RPA1. Biochemistry 48: 7473–7481.

Olson, E., C. J. Nievera, V. Klimovich, E. Fanning, and X. Wu, 2006 RPA2 is a direct downstream target for ATR to regulate the S-phase checkpoint. J. Biol. Chem. 281: 39517–39533.

Patrick, S. M., G. G. Oakley, K. Dixon, and J. J. Turchi, 2005 DNA damage induced hyperphosphorylation of Replication Protein A. 2. Characterization of DNA binding activity, protein interactions, and activity in DNA replication and repair. Biochemistry 44: 8438–8448.

Pellicioli, A., and M. Foiani, 2005 Signal transduction: how rad53 kinase is activated. Curr. Biol. CB 15: R769–R771.

Pellicioli, A., S. E. Lee, C. Lucca, M. Foiani, and J. E. Haber, 2001 Regulation of Saccharomyces Rad53 checkpoint kinase during adaptation from DNA damage-induced G2/M arrest. Mol. Cell 7: 293–300.

Psakhye, I., and S. Jentsch, 2012 Protein group modification and synergy in the SUMO pathway as exemplified in DNA repair. Cell 151: 807–820.

Rupnik, A., N. F. Lowndes, and M. Grenon, 2010 MRN and the race to the break. Chromosoma 119: 115–135.

Schramke, V., H. Neecke, V. Brevet, Y. Corda, G. Lucchini *et al.*, 2001 The set1Delta mutation unveils a novel signaling pathway relayed by the Rad53-dependent hyperphosphorylation of

Replication Protein A that leads to transcriptional activation of repair genes. Genes Dev. 15: 1845–1858.
Schramke, V., P. Luciano, V. Brevet, S. Guillot, Y. Corda *et al.*, 2004 RPA regulates telomerase action by providing Est1p access to chromosome ends. Nat. Genet. 36: 46–54.
Shi, W., Z. Feng, J. Zhang, I. Gonzalez-Suarez, R. P. Vanderwaal *et al.*, 2010 The role of RPA2 phosphorylation in homologous recombination in response to replication arrest. Carcinogenesis 31: 994–1002.
Sikorski, R. S., and P. Hieter, 1989 A system of shuttle vectors and yeast host strains designed for efficient manipulation of DNA in *Saccharomyces cerevisiae*. Genetics 122: 19–27.
Smith, J., L. M. Tho, N. Xu, and D. A. Gillespie, 2010 The ATM-Chk2 and ATR-Chk1 pathways in DNA damage signaling and cancer. Adv. Cancer Res. 108: 73–112.
Smolka, M. B., C. P. Albuquerque, S. Chen, and H. Zhou, 2007 Proteome-wide identification of in vivo targets of DNA damage checkpoint kinases. Proc. Natl. Acad. Sci. USA 104: 10364–10369.
Soulard, A., A. Cremonesi, S. Moes, F. Schutz, P. Jeno *et al.*, 2010 The rapamycin-sensitive phosphoproteome reveals that TOR controls protein kinase A toward some but not all substrates. Mol. Biol. Cell 21: 3475–3486.
Stark, C., T.-C. Su, A. Breitkreutz, P. Lourenco, M. Dahabieh *et al.*, 2010 *2010 PhosphoGRID: A Database of Experimentally Verified in Vivo Protein Phosphorylation Sites from the Budding Yeast Saccharomyces cerevisiae*. Database 2010: 1–13.
Sung, P., 1997 Function of yeast Rad52 protein as a mediator between Replication Protein A and the Rad51 recombinase. J. Biol. Chem. 272: 28194–28197.
Umezu, K., N. Sugawara, C. Chen, J. E. Haber, and R. D. Kolodner, 1998 Genetic analysis of yeast RPA1 reveals its multiple functions in DNA metabolism. Genetics 148: 989–1005.
Vassin, V. M., M. S. Wold, and J. A. Borowiec, 2004 Replication protein A (RPA) phosphorylation prevents RPA association with replication centers. Mol. Cell. Biol. 24: 1930–1943.
Vassin, V. M., R. W. Anantha, E. Sokolova, S. Kanner, and J. A. Borowiec, 2009 Human RPA phosphorylation by ATR stimulates DNA synthesis and prevents ssDNA accumulation during DNA-replication stress. J. Cell Sci. 122: 4070–4080.
Wang, H., J. Gao, A. H.-H. Wong, K. Hu, W. Li *et al.*, 2013 Rfa2 is specifically dephosphorylated by Pph3 in *Candida albicans*. Biochem. J. 449: 673–681.
Weinberg, D. H., K. L. Collins, P. Simancek, A. Russo, M. S. Wold *et al.*, 1990 Reconstitution of simian virus 40 DNA replication with purified proteins. Proc. Natl. Acad. Sci. USA 87: 8692–8696.
Williams, R. S., J. S. Williams, and J. A. Tainer, 2007 Mre11–Rad50–Nbs1 is a keystone complex connecting DNA repair machinery, double-strand break signaling, and the chromatin template. Biochem. Cell Biol. Biochim. Biol. Cell. 85: 509–520.
Wold, M. S., 1997 Replication protein A: a heterotrimeric, single-stranded DNA-binding protein required for eukaryotic DNA metabolism. Annu. Rev. Biochem. 66: 61–92.
Wold, M. S., and T. Kelly, 1988 Purification and characterization of Replication Protein A, a cellular protein required for in vitro replication of simian virus 40 DNA. Proc. Natl. Acad. Sci. USA 85: 2523–2527.
Wold, M. S., D. H. Weinberg, D. M. Virshup, J. J. Li, and T. J. Kelly, 1989 Identification of cellular proteins required for simian virus 40 DNA replication. J. Biol. Chem. 264: 2801–2809.
Wu, X., Z. Yang, Y. Liu, and Y. Zou, 2005 Preferential localization of hyperphosphorylated Replication Protein A to double-strand break repair and checkpoint complexes upon DNA damage. Biochem. J. 391: 473–480.
Zou, Y., Y. Liu, X. Wu, and S. M. Shell, 2006 Functions of human Replication Protein A (RPA): from DNA replication to DNA damage and stress responses. J. Cell. Physiol. 208: 267–273.

Communicating editor: J. A. Nickoloff

GENETICS

Supporting Information
http://www.genetics.org/lookup/suppl/doi:10.1534/genetics.114.173211/-/DC1

The DNA Damage Response and Checkpoint Adaptation in *Saccharomyces cerevisiae*: Distinct Roles for the Replication Protein A2 (Rfa2) N-Terminus

Padmaja L. Ghospurkar, Timothy M. Wilson, Amber L. Severson, Sarah J. Klein, Sakina K. Khaku, André P. Walther, and Stuart J. Haring

DOI: 10.1534/genetics.114.173211

Table S1 Yeast strains

Strain	Genotype	Source
RMY122	*MATα leu2-3,112 trp1-1 can1-100 ura3-1 his3-11,15 rad5-535 rfa1Δ::TRP1 rfa2Δ::TRP1*; this strain contains pJM132	(MANIAR *et al.* 1997)
RMY122-A	*MATa* derivative of RMY122 generated by mating-type switching	This study
RMY122-*mre11Δ*	*mre11Δ::kanMX* derivative of RMY122	This study
JKM179	*hoΔ MATα hmlΔ::ADE1 hmrΔ::ADE1 ade1-100 leu2-3,112 lys5 trp1::hisG' ura3-52 ade3::P_{GAL}-HO*	(LEE *et al.* 1998)
JKM139	*MATa* strain isogenic to JKM179	(LEE *et al.* 1998)
JKM181	*yku70Δ::URA3* derivative of JKM179	(LEE *et al.* 1998)
YSL31	*rfa1-t11* derivative of JKM179	(LEE *et al.* 1998)
YSL32	*yku70Δ::URA3 rfa1-t11* derivative of JKM179	(LEE *et al.* 1998)
AWY96	*rfa2-D_x* derivative of JKM179	This study
AWY99	*rfa2-D_x rfa1-t11* derivative of JKM179	This study
AWY295	*rfa2-D_x yku70Δ::URA3* derivative of JKM179	This study
AWY92	*rfa2-A_x* derivative of JKM179	This study
AWY108	*rfa2-A_x rfa1-t11* derivative of JKM179	This study
AWY292	*rfa2-A_x yku70Δ::URA3* derivative of JKM179	This study

Table S2 Plasmids

Plasmid	Description	Source
pJM132	pRS416 containing the *RFA1*, *RFA2*, and *RFA3* genes and their native promoters	(MANIAR *et al.* 1997)
pJM218	YCp50 containing *RFA2*	(MANIAR *et al.* 1997)
pGDB-C3	Yeast two-hybrid vector containing the Gal4 DNA binding domain (DB)	(JAMES *et al.* 1996)
pGDB-C3-*RFA2*	pGDB-C3 containing *RFA2* cDNA	This study
pGDB-C3-*rfa2*-D_x	pGDB-C3-*RFA2* with replacement of the N-terminus coding region with a 0.1 kbp *Eco*RI-*Hpa*I fragment produced by annealing primers AspA-E; the *rfa2*-D_x allele consists of all serines (S)/threonines (T) within the first 34 amino acids mutated to aspartic acids (D)	This study
pGDB-C3-*rfa2*-A_x	pGDB-C3-*RFA2* with replacement of the N-terminus coding region with a 0.1 kbp *Eco*RI-*Hpa*I fragment produced by annealing primers AlaA-E; the *rfa2*-A_x allele consists of all S/T within the first 34 amino acids mutated to alanines (A)	This study
pRS315-*RFA2*-Δpromoter	pRS315 with insertion of a 0.9 kbp *Eco*RI-*Hin*dIII fragment from pGDB-C3-*RFA2* containing *RFA2* cDNA	This study
pRS315-*rfa2*-D_x-Δpromoter	pRS315 with insertion of a 0.9 kbp *Eco*RI-*Hin*dIII fragment from pGDB-C3-*rfa2*-D_x containing *rfa2*-D_x cDNA	This study
pRS315-*rfa2*-A_x-Δpromoter	pRS315 with insertion of a 0.9 kbp *Eco*RI-*Hin*dIII fragment from pGDB-C3-*rfa2*-A_x containing *rfa2*-A_x cDNA	This study
pAW07	pRS315-*RFA2*-Δpromoter with insertion of the 0.6 kbp *Sac*II-*Nco*I-digested PCR fragment containing the native *RFA2* promoter	This study
pAW08	pRS315-*rfa2*-D_x-Δpromoter with insertion of the 0.6 kbp *Sac*II-*Nco*I-digested PCR fragment containing the native *RFA2* promoter	This study
pAW09	pRS315-*rfa2*-A_x-Δpromoter with insertion of the 0.3 kbp *Bam*HI-*Nco*I-digested PCR fragment containing the native *RFA2* promoter	This study
pAW10	pRS315-*rfa2*-ΔN_x-Δpromoter with insertion of the 0.6 kbp *Sac*II-*Nco*I-digested PCR fragment containing the native *RFA2* promoter	This study
pAW11	pRS306 with insertion of the 1.2 kbp *Bam*HI-*Hin*dIII fragment from pAW08 containing the native *RFA2* promoter and *rfa2*-D_x	This study
pAW12	pRS306 with insertion of the 1.2 kbp *Bam*HI-*Hin*dIII fragment from pAW09 containing the native *RFA2* promoter and *rfa2*-A_x	This study
pPLG1	pRS315-*RFA2* containing a S3D mutation to generate *rfa2*-D_{i3}	This study
pPLG2	pRS315-*RFA2* containing a S11D mutation to generate *rfa2*-D_{i11}	This study
pPLG3	pRS315-*RFA2* containing a S12D mutation to generate *rfa2*-D_{i12}	This study
pPLG4	pRS315-*RFA2* containing a T14D mutation to generate *rfa2*-D_{i14}	This study
pPLG5	pRS315-*RFA2* containing a S21D mutation to generate *rfa2*-D_{i21}	This study
pPLG6	pRS315-*RFA2* containing a S23D mutation to generate *rfa2*-D_{i23}	This study
pPLG7	pRS315-*RFA2* containing a S27D mutation to generate *rfa2*-D_{i27}	This study

Plasmid	Description	Source
pPLG8	pRS315-*RFA2* containing a S30D mutation to generate *rfa2-*D_{i30}	This study
pPLG9	pRS315-*RFA2* containing a T32D mutation to generate *rfa2-*D_{i32}	This study
pPLG10	pRS315-*RFA2* containing a T34D mutation to generate *rfa2-*D_{i34}	This study
pPLG11	pRS315-*RFA2* containing a T38D mutation to generate *rfa2-*D_{i38}	This study
pPLG12	pRS315-*RFA2* containing a S3A mutation to generate *rfa2-*A_{i3}	This study
pPLG13	pRS315-*RFA2* containing a S11A mutation to generate *rfa2-*A_{i11}	This study
pPLG14	pRS315-*RFA2* containing a S12A mutation to generate *rfa2-*A_{i12}	This study
pPLG15	pRS315-*RFA2* containing a T14A mutation to generate *rfa2-*A_{i14}	This study
pPLG16	pRS315-*RFA2* containing a S21A mutation to generate *rfa2-*A_{i21}	This study
pPLG17	pRS315-*RFA2* containing a S23A mutation to generate *rfa2-*A_{i23}	This study
pPLG18	pRS315-*RFA2* containing a S27A mutation to generate *rfa2-*A_{i27}	This study
pPLG19	pRS315-*RFA2* containing a S30A mutation to generate *rfa2-*A_{i30}	This study
pPLG20	pRS315-*RFA2* containing a T32A mutation to generate *rfa2-*A_{i32}	This study
pPLG21	pRS315-*RFA2* containing a T34A mutation to generate *rfa2-*A_{i34}	This study
pPLG22	pRS315-*RFA2* containing a T38A mutation to generate *rfa2-*A_{i38}	This study
pPLG23	pRS315-*RFA2* containing S3A, S11A, S12A, and T14A mutations to generate *rfa2-*A_{m1}	This study
pPLG25	pRS315-*RFA2* containing S21A, S23A, and S27A mutations to generate *rfa2-*A_{m2}	This study
pPLG26	pRS315-*RFA2* containing S30A, T32A, T34A, and T38A mutations to generate *rfa2-*A_{m3}	This study
pPLG27	pRS315-*RFA2* containing S3A, S11A, S12A, T14A, S21A, S23A, and S27A mutations to generate *rfa2-*A_{m1+2}	This study
pPLG24	pRS315-*RFA2* containing S21A, S23A, S27A, S30A, T32A, T34A, and T38A to generate *rfa2-*A_{m2+3}	This study
pPLG28	pRS315-*RFA2* containing S3A, S11A, S12A, T14A, S30A, T32A, T34A, and T38A mutations to generate *rfa2-*A_{m1+3}	This study
pPLG29	pRS315-*RFA2* containing S3D, S11D, S12D, and T14D mutations to generate *rfa2-*D_{m1}	This study
pPLG30	pRS315-*RFA2* containing S21D, S23D, and S27D mutations to generate *rfa2-*D_{m2}	This study
pPLG31	pRS315-*RFA2* containing S30D, T32D, T34D, and T38D mutations to generate *rfa2-*D_{m3}	This study
pPLG32	pRS315-*RFA2* containing S3D, S11D, S12D, T14D, S21D, S23D, and S27D mutations to generate *rfa2-*D_{m1+2}	This study
pPLG33	pRS315-*RFA2* containing S21D, S23D, S27D, S30D, T32D, T34D, and T38D to generate *rfa2-*D_{m2+3}	This study

Plasmid	Description	Source
pPLG34	pRS315-*RFA2* containing S3D, S11D, S12D, T14D, S30D, T32D, T34D, and T38D mutations to generate *rfa2-D*$_{m1+3}$	This study
pRS313-*RFA1*	pRS313 with insertion of a 2.6 kbp *Bam*HI-*Hin*dIII fragment from pJM132 containing *RFA1* and its native promoter	This study
pRS313-*rfa1-t11*	pRS313-*RFA1* with insertion of a 2.0 kbp *Age*I-*Hin*dIII fragment from pKU2-*rfa1-t11* containing the *rfa1-t11* (K45E) allele	This study
pRS313-*rfa1-S178A*	pRS313-*RFA1* containing the *rfa1-S178A* mutation generated by *in vitro* site-directed mutagenesis	This study
pRS313-*rfa1-S178D*	pRS313-*RFA1* containing the *rfa1-S178D* mutation generated by *in vitro* site-directed mutagenesis	This study
pRS315-*rfa2-S122A*	pAW07 containing the *rfa2-S122A* mutation generated by *in vitro* site-directed mutagenesis	This study
pRS315-*rfa2-S122D*	pAW07 containing the *rfa2-S122D* mutation generated by *in vitro* site-directed mutagenesis	This study

Table S3 Primers

Primer Name	Sequence (5′→3′)[a]	Notes
AspA	AATTCACCATGGCAGACTATCAACCATATAACGAATATGACGACGTAGACGGCGGTGG	AspC, AspD, and AspE are complementary primers to AspA and AspB
AspB	CTTTGAGAACGATGAGGACCGCCCGGGTGATGGGGAGGACGAAGATAACGATAGAGTT	
AspC	AACTCTATCGTTATCTTCGTCCTCCCCATCACCCGG	
AspD	GCGGTCCTCATCGTTCTCAAAGCCACCGCCGTCTACGTCG	
AspE	TCATATTCGTTATATGGTTGATAGTCTGCCATGGTG	
AlaA	CATGGCAGCTTATCAACCATATAACGAATATGCTGCTGTAGCTGGCGGTGGCTT	AlaC, AlaD, and AlaE are complementary primers to AlaA and AlaB
AlaB	TGAGAACGCTGAGGCTCGCCCAGGTGCTGGGGAGGCTGAAGCTAACGCTAGAGTT	
AlaC	AACTCTAGCGTTAGCTTCAGCCTCCCCA	
AlaD	GCACCTGGGCGAGCCTCAGCGTTCTCAAAGCCACCGCCAGCTACAGCAGC	
AlaE	ATATTCGTTATATGGTTGATAAGCTGC	
-PR-R1	AATAGGCGTATCACGAGGCC	Used to amplify *RFA2* promoter from pJM218
-PR-NcoI	GGTTGCCATGGTGTATATGCTTAAACTAGCC	
rfa2-S122D-BstEII	CTTCTGGTAAAGGTTATGGTGACCAAGTCGCCCAACAATTTG	*rfa2-S122D*; generates *Bst*EI site
rfa2-S122A-BsaHI	CTCTTCTGGTAAAGGTTATGGCGCCCAAGTCGCCCAACAATTTG	*rfa2-S122A*; generates *Bsa*HI site
pEG202-rfa1-S178A-F	CGCCAATGAAAACCCTAATGCTCAGAAAACCAGACCAATTTTTGCCATCG	*rfa1-S178A*; generates *Dde*I site
pEG202-rfa1-S178D-F	CGCCAATGAAAACCCTAATGATCAAAAAACCAGACCAATTTTTGCCATCG	*rfa1-S178D*; generates *Dpn*I site
rfa2-S3D-remake	TTAAGCATATACAAAATGGCAGATTATCAACCATATAAC	*rfa2-D$_{i3}$*; removes *Nco*I site
rfa2-S11D-FOR	CATATAACGAATATGATTCAGTAACGGGCG	*rfa2-D$_{i11}$*; removes *Ssp*I site
rfa2-S12D-FOR	CCATATAACGAATATAGTGATGTAACGGGCGGTG	*rfa2-D$_{i12}$*; removes *Ssp*I site
rfa2-T14D-FOR	GAATATTCATCAGTAGATGGCGGTGGCTTTGAG	*rfa2-D$_{i14}$*; generates *Bcc*I site
rfa2-S21D-FOR	GGCTTTGAGAACGACGAGAGTCGCCCAGGTAGTG	*rfa2-D$_{i21}$*; generates *Psh*AI site
rfa2-S23D-remake	GTGGCTTTGAGAACTCAGAGGATCGCCCAGGTAGTG	*rfa2-D$_{i23}$*; removes *Dde*I site
rfa2-S27D-FOR	GTCCCGCCCAGGTGATGGGGAGTCGGAAAC	*rfa2-D$_{i27}$*; generates *Bcc*I site
rfa2-S30D-FOR	GTCCCGCCCAGGATCCGGGGAGGATGAAACTAACACTAG	*rfa2-D$_{i30}$*; generates *Bam*HI site
rfa2-T32D-remake	GGGGAGTCGGAAGATAACACTCGAGTTAACACCTTG	*rfa2-D$_{i32}$*; generates *Xho*I site

Primer Name	Sequence (5′→3′)[a]	Notes
rfa2-T34D-FOR	GTCGGAAACTAACGATAGAGTAAACACCTTGACAC	*rfa2-D*$_{i34}$; removes *Hpa*I site
rfa2-T38D-remake	GAAACTAACACTCGAGTTAACGATTTGACACCTGTGACG	*rfa2-D*$_{i38}$; generates *Xho*I site
rfa2-S3A-FOR	TTAAGCATATACAAAATGGCAGCTTATCAACCATATAAC	*rfa2-A*$_{i3}$; removes *Nco*I site
rfa2-S11A-FOR	CATATAACGAATATGCTTCAGTAACGGGCG	*rfa2-A*$_{i11}$; removes *Ssp*I site
rfa2-S12A-FOR	CCATATAACGAATATTCAGCTGTAACGGGCGGTG	*rfa2-A*$_{i12}$; generates *Pvu*II site
rfa2-T14A-FOR	GAATATTCATCAGTAGCCGGCGGTGGCTTTGAG	*rfa2-A*$_{i14}$; generates *Nae*I site
rfa2-S21A-FOR	GGCTTTGAGAACGCTGAGAGTCGACCAGGTAGTGGGGAG	*rfa2-A*$_{i21}$; generates *Sal*I site
rfa2-S23A-FOR	GTGGCTTTCAGAACTCAGAGGCCCGCCCAGGTAGTG	*rfa2-A*$_{i23}$; removes *Dde*I site
rfa2-S27A-FOR	GTCCCGCCCAGGTGCCGGCGAGTCGGAAACTAAC	*rfa2-A*$_{i27}$; generates *Nae*I site
rfa2-S30A-FOR	GTCCCGCCCAGGATCCGGGGAGGCTGAAACTAACACTAG	*rfa2-A*$_{i30}$; generates *Bam*HI site
rfa2-T32A-FOR	GGGGAGTCGGAAGCTAACACTCGAGTTAACACCTTG	*rfa2-A*$_{i32}$; generates *Xho*I site
rfa2-T34A-FOR	GTCGGAAACTAACGCTAGAGTAAACACCTTGACAC	*rfa2-A*$_{i34}$; removes *Hpa*I site
rfa2-T38A-FOR	GAAACTAACACTCGAGTTAACGCGTTGACACCTGTGACG	*rfa2-A*$_{i38}$; generates *Xho*I site
rfa2-Asp(3,11,12,14)	ATATACACCATGGCAGATTATCAACCATATAACGAATATGATGATGTAGATGGCGGTGGC	*rfa2-D*$_{m1}$; removes *Ssp*I site
rfa2-Asp(21,23,27,30,32,34)	TTTGAGAACGACGAGGATCGCCCAGGTGATGGGGAGGATGAAGATAACGATAGAGTTAAC	*rfa2-D*$_{m1+m2}$; generates *Bcc*I site
rfa2-Asp(21,23,27)	TTTGAGAACGACGAGGATCGCCCAGGTGATGGGGAGTCGGAAACTAAC	*rfa2-D*$_{m2}$; generates *Bcc*I site
rfa2-Asp(30,32,34)	CGCCCAGGTAGTGGGGAGGATGAAGATAACGATAGAGTTAACACCTTGACA	*rfa2-D*$_{m3}$
rfa2-Ala(3,11,12,14)	ATATACACCATGGCAGCTTATCAACCATATAACGAATATGCTGCTGTAGCCGGCGGTGGC	*rfa2-A*$_{m1}$; removes *Ssp*I site
rfa2-Ala(21,23,27,30,32,34)	TTTGAGAACGCTGAGGCCCGCCCAGGTGCCGGGGAGGCTGAAGCTAACGCTAGAGTTAAC	*rfa2-A*$_{m1+m2}$; generates *Bgl*I site
rfa2-Ala(21,23,27)	TTTGAGAACGCTGAGGCCCGCCCAGGTGCCGGGGAGTCGGAAACTAAC	*rfa2-A*$_{m2}$; generates *Nci*I site
rfa2-Ala(30,32,34)	CGCCCAGGTAGTGGGGAGGCTGAAGCTAACGCTAGAGTTAACACCTTGACA	*rfa2-A*$_{m3}$
rfa2-DeltaN(3-14)	TTAAGCATATACACCATGGCAGGCGGTGGCTTTGAGAACTCT	*rfa2-*Δ*N*$_1$
rfa2-DeltaN(21-27)	ACGGGCGGTGGCTTTGAGAACGGGGAGTCGGAAACTAACACT	*rfa2-*Δ*N*$_2$
rfa2-DeltaN(30-40)	TCCCGCCCAGGTAGTGGGGAGCCTGTGACGATCAAACAAATT	*rfa2-*Δ*N*$_3$

[a] Underlined bases indicate serine/threonine to aspartic acid or alanine substitutions.

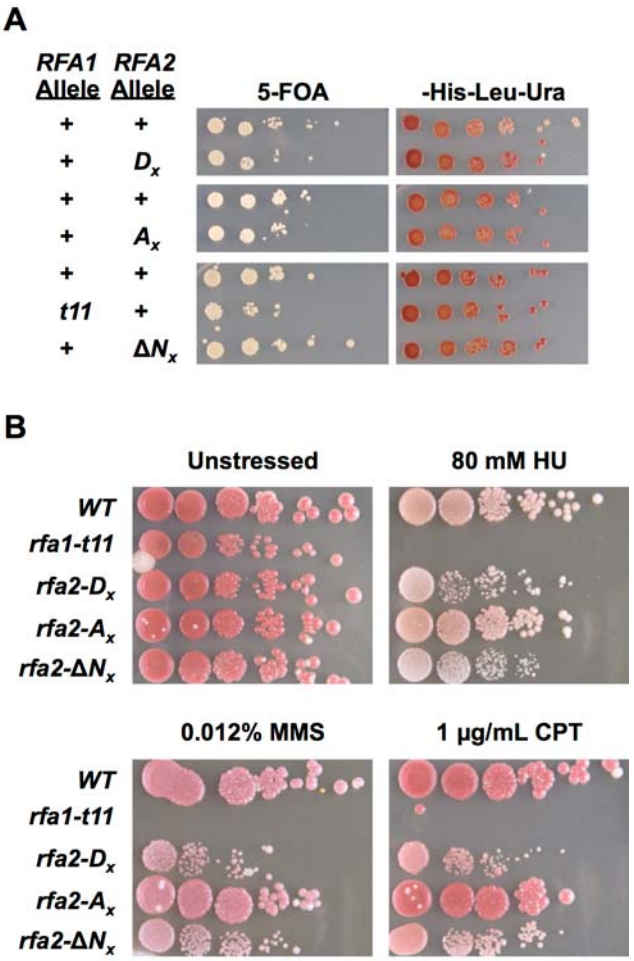

Figure S1 Phenotypic analysis of *rfa2* "extensive" (*rfa2*$_x$) mutants in response to DNA damage.

[A] Measuring the viability of rfa2 extensive mutants. Cells were grown overnight, sonicated, counted, and diluted to 2x10^6 cells/mL. Ten-fold serial dilutions were made, and 5 µL of each dilution for each strain were spotted onto SD-His-Leu-Ura (selective for cells containing all three plasmids), and 5-FOA (selective for cells that have lost pJM132). Growth on 5-FOA indicates that a particular cDNA or mutant form of *RFA2* can complement the *rfa2*Δ on the chromosome, which will result in the "shuffling out" of pJM132 (*URA3* plasmid containing WT *RFA1* and *RFA2* genes). The *RFA1* allele and *RFA2* allele contained on the two plasmids "shuffled in" are denoted. Symbols: *+* = *WT*; *t11* = *rfa1-t11*; D_x, A_x, or ΔN_x = extensive mutant forms shown in Figure 2B.

[B] DNA damage assay of the rfa2 extensive mutants. DNA damage assays were performed on *rfa2* extensive mutants (Figure 2B; 2D) as described in Figure 1B.

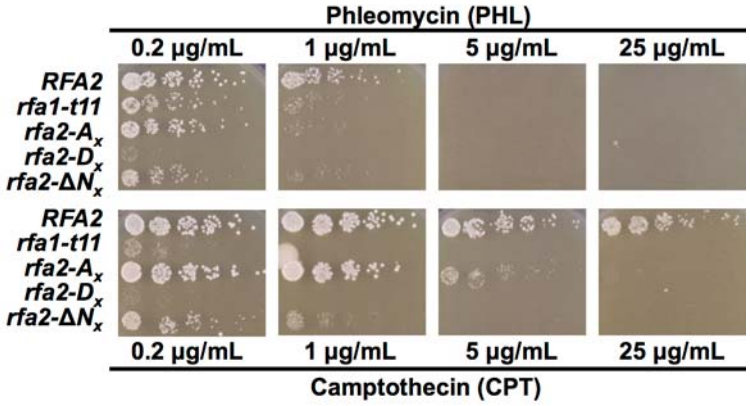

Figure S2 Phenotypic analysis of *rfa2* "extensive" (*rfa2*$_x$) mutants in response to DNA damage in the JKM179 background (strains used for adaptation studies).

DNA damage assays were performed on *rfa2* extensive mutants in the JKM179 background as described in Figure 1B.

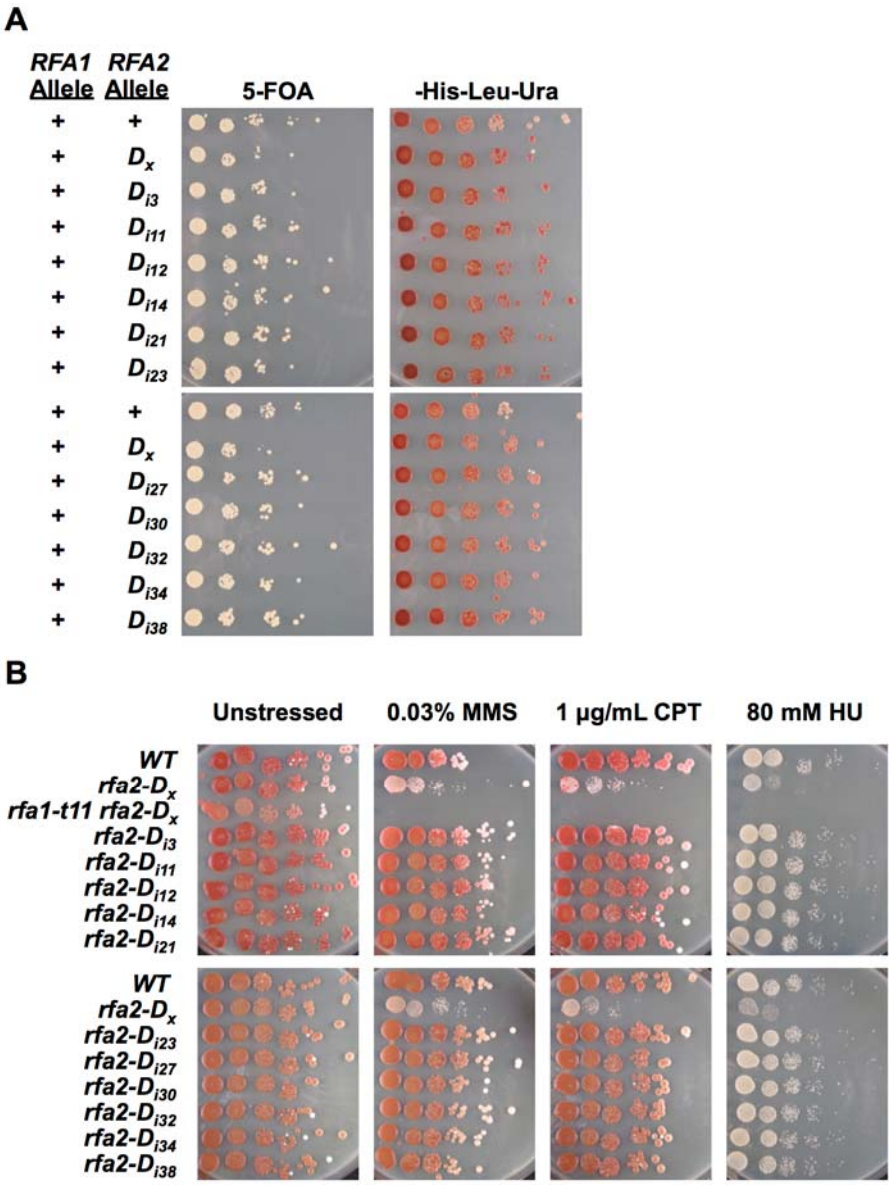

Figure S3 Viability and DNA damage sensitivity of *rfa2* "individual" mutants (*rfa2*$_i$).

[A] Plasmid shuffle to recover viable rfa2-D$_i$ mutants. The viability of *rfa2* individual mutants was examined by plasmid shuffle as described in Figure S1A. The number following the subscript *i* indicates the residue mutated (see Figure 2B).

[B] DNA damage assays for rfa2-D$_i$ mutants. Plasmid shuffle was used to recover *rfa2-D$_i$* mutant cells (Figure S4A). These mutant cells were then grown and assayed for resistance to DNA damaging agents as described in Figure 1B.

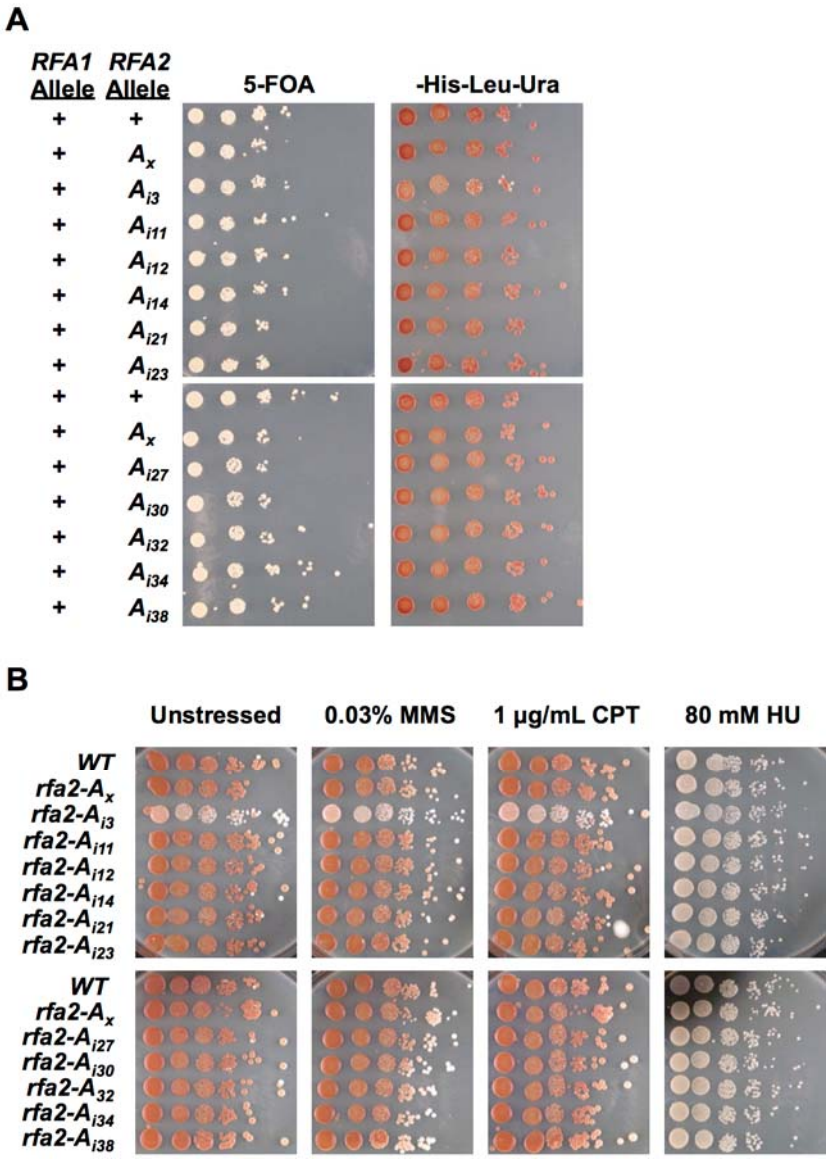

Figure S4 Viability and DNA damage sensitivity of *rfa2* "individual" mutants (*rfa2*$_i$).

[A] Plasmid shuffle to recover viable rfa2-A$_i$ mutants. The viability of *rfa2* individual mutants was examined by plasmid shuffle as described in Figure S1A. The number following the subscript *i* indicates the residue mutated (see Figure 2B).

[B] DNA damage assays for rfa2-A$_i$ mutants. Plasmid shuffle was used to recover *rfa2-A$_i$* mutant cells (Figure S3A). These mutant cells were then grown and assayed for resistance to DNA damaging agents as described in Figure 1B.

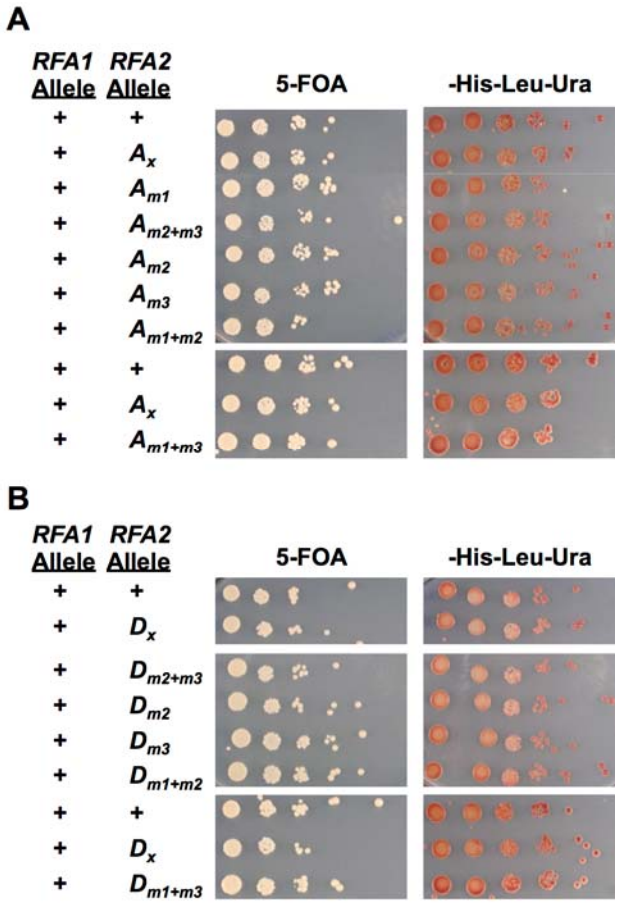

Figure S5 Viability of *rfa2* multi-mutants (*rfa2*$_m$).

The viability of *rfa2* multi-mutants was examined by plasmid shuffle as described in Figure S1A. Alanine multi-mutants (A_m) and aspartic acid mutants (D_m) are shown in *[A]* and *[B]*, respectively. The number following the subscript *m* indicates the N-terminal subregion that was mutated (see Figure 4A). *rfa2*-D_{m1} (not shown) was recovered on 5-FOA and grew indistinguishably to other multi-mutants.